NASA Contractor Report 3460

Experimental and Theoretical Study of Three Interacting, Closely-Spaced, Sharp-Edged 60° Delta Wings at Low Speeds

H. F. Faery, Jr., J. K. Strozier,
and J. A. Ham

OCTOBER 1981

NASA

NASA Contractor Report 3460

Experimental and Theoretical Study of Three Interacting, Closely-Spaced, Sharp-Edged 60° Delta Wings at Low Speeds

H. F. Faery, Jr., J. K. Strozier,
and J. A. Ham
United States Military Academy
West Point, New York

Prepared in cooperation with
NASA Langley Research Center
and funded by the
United States Military Academy

National Aeronautics
and Space Administration

**Scientific and Technical
Information Branch**

1981

EXPERIMENTAL AND THEORETICAL STUDY OF THREE INTERACTING, CLOSELY-SPACED, SHARP-EDGED 60^0 DELTA WINGS AT LOW SPEEDS

Henry F. Faery, Jr.*, James K. Strozier**, and Johnnie A. Ham***

SUMMARY

An investigation was conducted using the United States Military Academy's (USMA) computer facilities and subsonic wind tunnel to determine the lift, drag, and pitching moment characteristics of three interacting delta wings. In particular, the study was designed to determine the effects caused by varying the locations of two smaller delta wings (called sub-wings here) beneath a larger delta main wing. The tests were conducted at angles of attack up to 34^0 and a Reynolds number of 2.85×10^6 per meter (8.68×10^5 per foot). The three wings involved in the study had a leading edge sweep angle of 60^0 with a sharp leading edge.

The results of this study indicate that lateral separation of the two sub-wings produces no significant changes in the aerodynamic forces and moments of the entire three-wing assembly. However, vertical displacement and fore-aft variations did show significant changes. Increasing the vertical separation of the sub-wings from the main wing produced a 23.1% increase in maximum lift coefficient over that for a minimum separation. Longitudinal stability was also increased by increasing vertical separation. Results of fore-aft variation in sub-wing location showed that the maximum lift coefficient increased as the

---

*LTC, US Army; Associate Professor, U.S. Military Academy.
**COL, US Army; Associate Professor, U.S. Military Academy.
***2LT, US Army; formerly undergraduate student, U.S. Military Academy.

sub-wings were moved aft and the initial lift curve slope increased. An aft location also produced improvements in the longitudinal stability. Results of a computer study using a NASA-developed vortex lattice code supported the experimental conclusions.

INTRODUCTION

Over the past several years, the NASA has been studying a concept for a possible future space transportation system (refs. 1-3), one that might replace the current space shuttle system. This concept has been called Spacejet. Spacejet is a totally reusable system that would conceptually use both turbojets and rocket engines. The turbojets would provide the necessary thrust for horizontal take-off and trajectory initialization, after which they would stage, leaving the rocket engine of the orbiter to complete the orbital insertion. The boosters, in the meantime, would fly back to a normal landing and could begin preparation for later reuse. A part of this sequence is shown in figure 1, and an artist's concept of a possible Spacejet configuration is shown in figure 2.

The Spacejet model that has been tested by the NASA consists of a main strake-wing and two smaller strake-wings (called here sub-wings or booster wings) attached to the turbojet engine nacelles as shown in figure 3. All three wings have a delta planform shape, and two of them, the sub-wings, are mounted below the main wing. During take-off, all of these wings depend on leading-edge vortex lift (ref. 4) to get the vehicle airborne. Therefore, it is imperative to understand the interaction between the upper and lower surface vortex systems and to determine the relative locations of the wings which appear most advantageous from an aerodynamic standpoint. These exact interactions are not properly

handled by current theoretical analysis, though the vortex lattice method coupled with the suction analogy is employed herein to make state-of-the-art theoretical estimates (refs. 5 and 6), hence wind tunnel experiments are sought to provide the best initial answers. In fact, one such study was reported by the NASA as reference 3 and focused on the aerodynamics of take-off performance and transonic drag.

In light of the unknowns associated with such a program, the present investigation was undertaken as a baseline study to determine the effects of wing interference on the longitudinal aerodynamic forces and moments. The departure point for the study is the delta wing. The advantages associated with the delta are quite compatible with an orbiter undergoing horizontal take-off and orbital return. These potential benefits include: the large amount of available lift during the take-off phase; acceptable high angle-of-attack capability, useful also in the reentry configuration; and the abundance of experimental information on delta wings to evaluate theoretical predictions and to indicate aspects that require special attention, theoretically or experimentally.

The aerodynamic parameter of prime interest for this series of tests was $C_{L,max}$ since it is crucial to the take-off phase of any configuration. For this study it is assumed that sufficient take-off thrust is available, hence the drag coefficient does not assume its usual importance. In other words, this study was primarily interested in determining the most advantageous configuration for producing maximum take-off lift. By the same token, positive stability is desirable, but not crucial to these tests.

A simplified version of the Spacejet geometry was tested in a subsonic wind tunnel at the U.S. Military Academy. The model consisted of three flat plate

delta wings, one main wing and two sub-wings, each having a 60^0 leading edge sweep with a sharp leading edge. Testing concentrated on determining the effects which forward, lateral, and vertical variations in sub-wing position had on the configuration lift, drag, and pitching moment. This report contains an account of the research findings.

SYMBOLS

The position reference-axis system used is shown in figure 4. The longitudinal data are referred to the wind-axis system. The axis origin is at the moment reference position located at the centroid of the main wing as also shown on this figure. Dimensional values are given in the International System of Units and the U. S. Customary Units.

b	main wing span, .264 m (.866 ft)
$\bar{c}$	mean aerodynamic chord of the main wing, .152 m (.5 ft)
C_D	drag coefficient, drag/$q_\infty S_{ref}$
$C_{D,o}$	drag coefficient at zero lift
C_L	lift coefficient, lift/$q_\infty S_{ref}$
$C_{L,max}$	maximum lift coefficient
C_{L_α}	rate of change of lift coefficient with angle of attack, per degree
C_m	pitching-moment coefficient, pitching-moment/$q_\infty S_{ref}\ \bar{c}$, taken about 50% $\bar{c}$.
L/D	lift to drag ratio
ℓ	typical length, see Table 1.
M_∞	free-stream Mach number

q_∞	free-stream dynamic pressure, N/m^2 (lb/ft^2)
R	Reynolds number
S_{ref}	reference area, equal to model main wing area, .0302 m^2 (.3247 ft^2)
$\bar{X},\bar{Y},\bar{Z}$	reference axis system (see figure 4 for positive directions)
$\bar{x},\bar{y},\bar{z}$	distances along the reference axes, m (ft)
X	normalized position of sub-wing along longitudinal axis, $\bar{x}/(b/2)$ (Note that model configuration is always symmetrical)
Y	normalized position of right sub-wing along lateral axis, $\bar{y}/(b/2)$ (Note that model configuration is always symmetrical)
Z	normalized position of sub-wing along vertical axis, $\bar{z}/(b/2)$ (Note that model configuration is always symmetrical)
α	angle of attack, degrees

MODEL DESCRIPTION AND TEST TECHNIQUE

Model

Figure 5 presents a sketch of the model used for this investigation, and figure 6 shows two views of a typical installation. The wings had a sweep angle of 60^0 and were made from 0.3175-cm (1/8-inch) thick aluminum with a 7.5^0 taper normal to the leading edges. The root chord of the main wing was 22.86 cm (9.0 inches) and 11.43 cm (4.5 inches) for each sub-wing. Struts mounted on the rear were adjusted to permit testing of the various separations of the sub-wings with respect to each other and with respect to the main wing. A streamlined housing was attached to the main wing to hold a sting-mounted six component strain gage balance. The drag associated with the base of the housing has been eliminated by tapering it to a sharp edge, and the chamber drag has been accounted for in the presented data.

Experimental Procedure

All experiments were conducted in the USMA Subsonic Wind Tunnel at 44.7 m/s (146.7 fps), M_∞ = .13, with R = 2.85 x 10^6 per meter (8.68 x 10^5 per foot). The tunnel is a low-speed, continuous, single-return system having a closed .51 m x .76 m (1.667 ft x 2.5 ft) rectangular test section. The sting-mounted model was tested at angles of attack from 0^0 to 34^0. The model size and mounting system kept the model in the center portion of the test section, ensuring that the model did not enter a region of flow in which there was more than a 2% variation from the free-stream mean velocity. Furthermore, this positioning kept the tunnel floor and ceiling effects from becoming significant. The angle of attack was measured by an optical setting device that was accurate to 0.5^0.

A NASA CF_4-2 six component balance supplied the normal, axial, and pitching moment measurements in digital readout form. Correction factors for wake blockage and tunnel wall interference were applied to the data. In addition, the effects of temperature change on density and the test section turbulence (factor 1.04) were taken into account. The wings were zeroed at an angle of attack where the normal force was zero to account for possible flow angularities.

The first configuration tested was the main wing alone. This was done for comparison to previous delta wing work and used as a baseline for this study. The next configurations tested were the sub-wings at separations of Y = 0, 0.0481, 0.0962, 0.1443, and 0.1925. The remaining test configurations are shown in Table 1.

From drawings supplied by the NASA for the Spacejet model (ref. 3) it was determined that the USMA generic model could cover the entire range of the NASA settings with the exception of the longitudinal variation. (See Table 2 for a

comparison of the settings.) The sub-wings of the USMA model cannot be placed as far forward along the longitudinal axis as the NASA model; however, the USMA model does allow settings that are further rearward.

The separations used herein are normalized to the half-span of the main wing. All force and moment coefficients of the main wing, sub-wings, and the combined configuration are normalized to the main wing planform area and the moments are taken about the centroid of the main wing, .152 m (.500 ft) behind the apex.

RESULTS AND DISCUSSION

Experimental

Main Wing and Sub-Wings

In order to establish a baseline for this study the main wing was tested alone. Figure 7 shows this data and compares the results to published data found in the literature. It is obvious that the USMA model apparently provides results that are slightly above what appears to be a "norm" from past tests. The curves plotted from references 7-9 (and unpublished data by Yip & Faery) illustrate one important reality - the same type model, tested in different tunnels at different times using different equipment and experimenters, provides different results. There appears to be an approximately 10% scatter in this data. $C_{L,max}$ from the USMA model falls well within this scatter. It is only 6% above the "norm". However, the straight line portion of the lift curve slope appears to be outside the scatter band. Therefore, absolute values obtained from these tests appear to be about 6% high at the higher angles of attack. It is felt that the vibration levels in the USMA system are likely responsible for

a major portion of this variation. This does not, however, invalidate the comparative results; in particular, the trends obtained are considered reliable.

The sub-wing pair was tested by itself (main wing not present) at lateral separations of Y = 0 (wingtips touching), 0.0481, 0.0962, 0.1443, and 0.1925. The differences in the results, however, were so insignificant that only the Y = 0 separation is plotted (figure 8). It should be noted that the $C_{L,max}$ occurs at the same angle of attack as the main wing and each point is located at approximately half the main wing C_L value, which should be expected.

In the figures that follow, all contain the basic delta wing data for reference, since that configuration can be thought of as a limiting case of the complete configuration with X = Y = Z = 0.

Effect of Vertical Separation

Figure 9 presents the effect of sub-wing vertical separation (Z = 0.0962, 0.1925, 0.3849, 0.5774, 0.7698) by examining the longitudinal aerodynamic results obtained for the configurations with the sub-wing inboard tips touching and the sub-wing trailing edges aligned with that of the main wing. From the C_L curves on figure 9(a) there is seen to be a significant increase in $C_{L,max}$ that results from moving the sub-wings away from the main wing. An increase of 23.1% was realized in going from Z = 0.0962 to Z = 0.7698. This trend was expected in that as the separation distance increases between the main wing and sub-wings, the vortex flow about the main wing would interfere less with the vortex pattern around the sub-wings and vice versa. In the limit as $Z \to \infty$ the sub-wings and main wing would experience no mutual interference. A

flow visualization test would be very useful to help understand the interference characteristics of these flow fields, particularly the leading edge vortex structure produced by both the main wing and sub-wings and their vortex breakdown characteristics for finite Z.

Figure 9(a) further shows there to be a dramatic increase in lift coefficient at each angle of attack as the vertical separation increases. The most significant change occurred between Z = 0.1925 and Z = 0.3849. Because of this nonlinear indicator, the remainder of the testing for lateral and longitudinal variations focused on these two vertical separations.

The drag is expected to be high for these configurations, on the order of $C_L \tan \alpha + C_{D,o}$, and the data are presented in figure 9(b). At C_L's that correspond to angles of attack $\leq 13^0$, the drag coefficient steadily increases with increasing separation. The curves show that at $C_L = 0$ there is an almost 77% increase in $C_{D,o}$ over this Z range. All of this increase can be attributed to the increased strut drag associated with its increased length required to reach the larger values of Z. In fact, calculations indicate that were the struts not present the $C_{D,o}$ will decrease slightly as the vertical separation increases. At angles of attack greater than 13^0, the trend reverses.

Another significant result of vertical separation is the increase in longitudinal stability shown in figure 9(c). This trend arises from the load center shift associated with the lift on each component, and the drag changes.

Effect of Longitudinal Variation

The longitudinal effects were investigated by moving the sub-wings forward and aft of the main wing trailing edge. Several different vertical separations

were also used. Figures 10 and 11 depict the results of the tests conducted at two different vertical separation distances, Z = .1925 and Z = .3849. Both vertical separations seem to indicate essentially the same trends, an increase in $C_{L,max}$ and $C_{L\alpha}$ and an increase in pitch stability as the sub-wings are moved rearward. The most significant results, however, occur at the smaller vertical separation (Z = .1925). At this position there is a 22% increase in $C_{L,max}$ with rearward movement of the sub-wings. In comparing the most forward position of the sub-wings with the results of the basic delta wing by itself, there is almost no improvement in $C_{L,max}$ and a degradation in the lift curve slope.

Unlike the results shown by vertical separation, there appears to be virtually no change in $C_{D,o}$ with longitudinal position of the sub-wings, nor would any be expected since the strut length remains constant. The only exception occurs when the sub-wings are in their most forward position at the smaller vertical separation. This anomaly does not appear to be easily explained. Perhaps flow visualization tests would provide some answers.

Effect of Lateral Separation

Figure 12 shows the effects on the longitudinal aerodynamic characteristics of moving the sub-wings laterally from a Y = 0 separation (wing tips touching) to a Y = .1925 separation. As shown, there is only a slight improvement in $C_{L,max}$ and longitudinal stability as the sub-wings are moved further outboard. Since increased lateral separation produces more leading edge exposure to undisturbed free stream air, one would expect less interference with the leading-edge vortices of the booster wings, and consequently the increased lift

measured. This does occur, but is limited; perhaps, due to the range of lateral separations investigated.

Theoretical Study

General Description

The vortex-lattice program documented in references 5 and 6, enables a theoretical study to be made of the effects of separation - vertical, longitudinal, and lateral - between the main and sub-wings on the total lift and pitching moment. The program can represent this configuration of main wing and sub-wings arranged in any symmetrical placement with respect to the main wing and between each other.

Effect of Vertical Separation

The results of the variation of vertical separation between main and sub-wings are shown in figure 13 for values of Z varying from .1925 to .9623. X and Y were both set at zero for this computation. As shown in the figure, increasing Z increased C_L, but the rate of increase decreases with increasing Z. For example, going from the basic delta (X = Y = Z = 0) to a Z = .1925 gave an 18.1% increase in C_L at $\alpha = 6^0$, whereas increasing Z from .7698 to .9623, the same increment, produces only a 2.5% increase in C_L at the same α.

Also of interest is the theoretical maximum increase in C_L. If the sub-wings were separated from the main wing and each other far enough so that the flow around each was not influenced by the flow around the others, each would act as an isolated delta. This would increase the C_L value by 50% over

that for the basic delta (since the area of each sub-wing is 25% of the main wing area). If this is plotted on the figure it would fall very close to the Z = .9623 line, indicating that this separation gives almost the maximum possible increase in C_L over the basic delta. This gives a measure as to the unfavorable interference experienced by the combination at smaller separation distances. It can also be seen that a Z value of .5774 gives a 38.2% increase in C_L over the basic delta ($\alpha = 6^0$), and this result is 76.4% of the theoretical noninterfering maximum. Since this vertical separation is approaching the maximum physical separation due to structural and other considerations of the wind tunnel model, further computer studies were restricted to this vertical separation.

Effect of Longitudinal Variation

Figure 14 shows the effect of longitudinal position on C_L. As mentioned previously, Z was set to 0.5774 and Y was set at zero. Moving the booster wings behind the trailing edge (negative X) gave a slight increase in C_L (approximately 2%) while movement forward gave negative or zero increase in C_L. Hence, C_L is almost insensitive to longitudinal repositioning of the sub-wings.

Effect of Lateral Separation

Figure 15 shows the effect of lateral separation on C_L for values of Y from 0 to .5774 with Z = .5774 and X = 0. It is noted that C_L increases with increasing Y. Furthermore, at Y = .5774 the theoretical results show an approximate 50% increase in C_L ($\alpha = 6^0$) over that for the basic delta. This is what

one would expect if the wings were flying in an interference-free flow field. In other words, this lateral separation theoretically produces the maximum lift increase which could be expected.

Separation Effects on Longitudinal Stability

Figure 16 shows the effect of the various separations on the pitching moment, C_m. Increasing Z (vertical separation), or Y (lateral separation), or decreasing X (rearward movement of sub-wing) causes the longitudinal stability to improve.

Comparison of Experimental and Theoretical Results

Figure 17 presents a comparison of the experimental and theoretical results on the basic delta wing alone. The theoretical curve is determined from the vortex-lattice computer code documented in references 5 and 6. The experimental lift curve of the main wing is in good agreement with this theoretical result, which includes the vortex lift effect, at the lower angles of attack, $\alpha \leq 18^0$. Naturally, as the angle of attack increases ($\alpha > 18^0$) and the leading-edge vortex breakdown becomes more severe, the tunnel results will deviate more from the theoretical values.

A comparison of Figures 9(a) and 13 indicates the same trend for an increasing vertical separation. For Z = .7698 and $\alpha = 10^0$, the VLM theory predicts a 40% increase in C_L over the basic delta wing, and the experimental results show a 36% increase. There is one significant difference, however, in the way

in which the increases occur. For example, in increasing Z from .1925 to .3849, theory shows an 8.6% increase in C_L, whereas data shows a 16.2% increase. Further increases in separation produce essentially the same results, a steadily decreasing increment in C_L improvement. Preliminary observations from a flow visualization study indicate that these disparate results are due to the character of the leading edge vortex flow over the outer edges of the two sub-wings. At small vertical separations ($Z \leq .1925$) it appears that the leading edge vortex from the outside edge of the sub-wing jumps to the main wing, causing a reduction in vortex lift effectiveness on the sub-wing, and very likely interfering with the lift development of the main wing. Whereas, for $Z > .1925$ there is a rapid increase in C_L for the complete model as the leading edge vortices begin to act on each of the components.

Figures 11(a) and 14 indicate that aft positioning of the sub-wings is more beneficial in terms of C_L improvement, although the differences at low angles of attack are not too significant.

Lateral separation effects can be compared using Figures 12(a) and 15. Moving the sub-wings further apart does increase C_L at each angle of attack, but there does not appear to be a significant shift associated with the lateral location.

Results from the NASA experiment on the Spacejet model indicate that lift is increased by increasing the vertical separation between the boosters and the main wing and by moving the boosters aft and further outboard.

An examination of figures 9(c), 10(c), 11(c), 12(c), and 16 provides an interesting correlation of pitching moment results. Although the experimental test configurations are not identical to the theoretical configurations presented on figure 16, a very valid comparison of trends is still possible.

Figure 16 indicates that increasing vertical separation will shift the C_m - C_L curve to a more positive slope, as will a movement of the sub-wings to a more aft longitudinal position. These same trends resulted from the wind tunnel study. The vortex lattice results also indicated a more significant shift toward positive pitch stability due to increasing lateral separation of the sub-wings. Figure 12c presents the same trend experimentally.

CONCLUSIONS

The longitudinal aerodynamic characteristics peculiar to a complex delta wing configuration having a 60^0 main wing and two smaller 60^0 delta sub-wings have been predicted theoretically and verified experimentally. It has been determined that the positioning of two sub-wings of delta shape beneath a main delta wing planform can have a significant effect on the lift, drag, and pitching-moment characteristics. Specific conclusions are as follows:

1. An increase in vertical separation between the main delta wing and the sub-wings showed the most significant results. Increasing vertical separation produces an increase in maximum lift coefficient and lift curve slopes, a decrease in drag coefficient at high lift coefficient, and an increase in the longitudinal stability.

2. Rearward movement of the sub-wings resulted in an increase in maximum lift coefficient and lift curve slope, a decrease in drag coefficient at high lift coefficients, and an increase in the longitudinal stability.

3. Lateral separation of the sub-wings produced no significant changes, although there were slight improvements in lift characteristics as the sub-wings were moved further apart.

4. The above results verify trends observed in preliminary work by NASA researchers on a complete space-shuttle type vehicle of similar wing design.

5. Theoretical results using a computer code based on vortex-lattice methods predict the same trends as outlined above. The theory, however, does not predict well the results associated with small vertical separations.

REFERENCES

1. Hepler, A. K., Zeck, H., Walker, W., and Scharf, W.: A Turbojet-Boosted Two-Stage-to-Orbit Space Transportation System Design Study, NASA CR-159018, April 1979.

2. Jackson, L. R., Martin, J. A., and Small, W. J.: A Fully Reusable, Horizontal Takeoff Space Transport Concept with Two Small Turbojet Boosters, NASA TM-74087, 1977.

3. Small, W. J., Riebe, G. D., and Taylor, A. H.: Aerodynamics of a Turbojet-Boosted Launch Vehicle Concept, AIAA Paper No. 80-0360, January 1980.

4. Polhamus, Edward C.: A Concept of the Vortex Lift of Sharp-Edge Delta Wings Based on a Leading-Edge-Suction Analogy, NASA TN D-3767, 1966.

5. Lamar, J. E. and Gloss, B. B.: Subsonic Aerodynamic Characteristics of Interacting Lifting Surfaces with Separated Flow Around Sharp Edges Predicted by a Vortex-Lattice Method, NASA TN D-7921, 1975.

6. Margason, R. J. and Lamar, J.E.: Vortex-Lattice FORTRAN Program for Estimating Subsonic Aerodynamic Characteristics of Complex Planforms, NASA TN D-6142, 1971.

7. Campbell, J. P., Johnson, J. L. Jr., and Hewes, D.E.: Low-Speed Study of the Effect of Frequency on the Stability Derivatives of Wings Oscillating in Yaw with Particular Reference to High Angle-of-Attack Conditions, NACA RM L55H05, 1955.

8. Wentz, W. H. Jr. and Kohlman, D. L.: Wind Tunnel Investigations of Vortex Breakdown on Slender Sharp-Edged Wings, NASA CR-98737, 1968.

9. Goodman, A. and Thomas, D. F. Jr.: Effects of Wing Position and Fuselage Size on the Low-Speed Static and Rolling Stability Characteristics of a Delta-Wing Model, NACA Report 1224, 1955.

Table 1. - Sub-wing Settings for USMA Model

Item	USMA Model Setting, ℓ cm (inches)	Normalized Setting, $\ell/b/2$
$\bar{x}_1$	- 0 (0)	0
$\bar{x}_2$	1.270 (0.50)	.0962
$\bar{x}_3$	2.540 (1.00)	.1925
$\bar{x}_4$	-1.270 (-0.50)	-.0962
$\bar{x}_5$	-2.540 (-1.00)	-.1925
$\bar{y}_1$	0 (0)	0
$\bar{y}_2$	0.635 (0.25)	.0481
$\bar{y}_3$	1.270 (0.50)	.0962
$\bar{y}_4$	1.905 (0.75)	.1443
$\bar{y}_5$	2.540 (1.00)	.1925
$\bar{z}_1$	1.270 (0.50)	.0962
$\bar{z}_2$	2.540 (1.00)	.1925
$\bar{z}_3$	5.080 (2.00)	.3849
$\bar{z}_4$	7.620 (3.00)	.5774
$\bar{z}_5$	10.160 (4.00)	.7698

Table 2. - Sub-wing Settings for NASA Model (Ref. 3) and USMA Model

	NASA Setting cm (inches)	Comparable USMA Setting cm (inches)	Actual USMA Setting cm (inches)
$\bar{x}_1$	3.429 (1.35)	2.057 (.81)	1.270 (.50)
$\bar{x}_2$	7.239 (2.85)	4.369 (1.72)	2.540 (1.0)
$\bar{x}_3$	11.049 (4.35)	6.655 (2.62)	-
$\bar{y}_1$	0 (0)	0 (0)	0 (0)
$\bar{y}_2$	2.921 (1.15)	1.753 (.69)	1.270 (.5) & 1.905 (.75)
$\bar{z}_1$	5.359 (2.11)	3.226 (1.27)	2.540 (1.0)
$\bar{z}_2$	6.883 (2.71)	4.140 (1.63)	5.080 (2.0)
$\bar{z}_3$	9.423 (3.71)	5.664 (2.23)	7.620 (3.0)

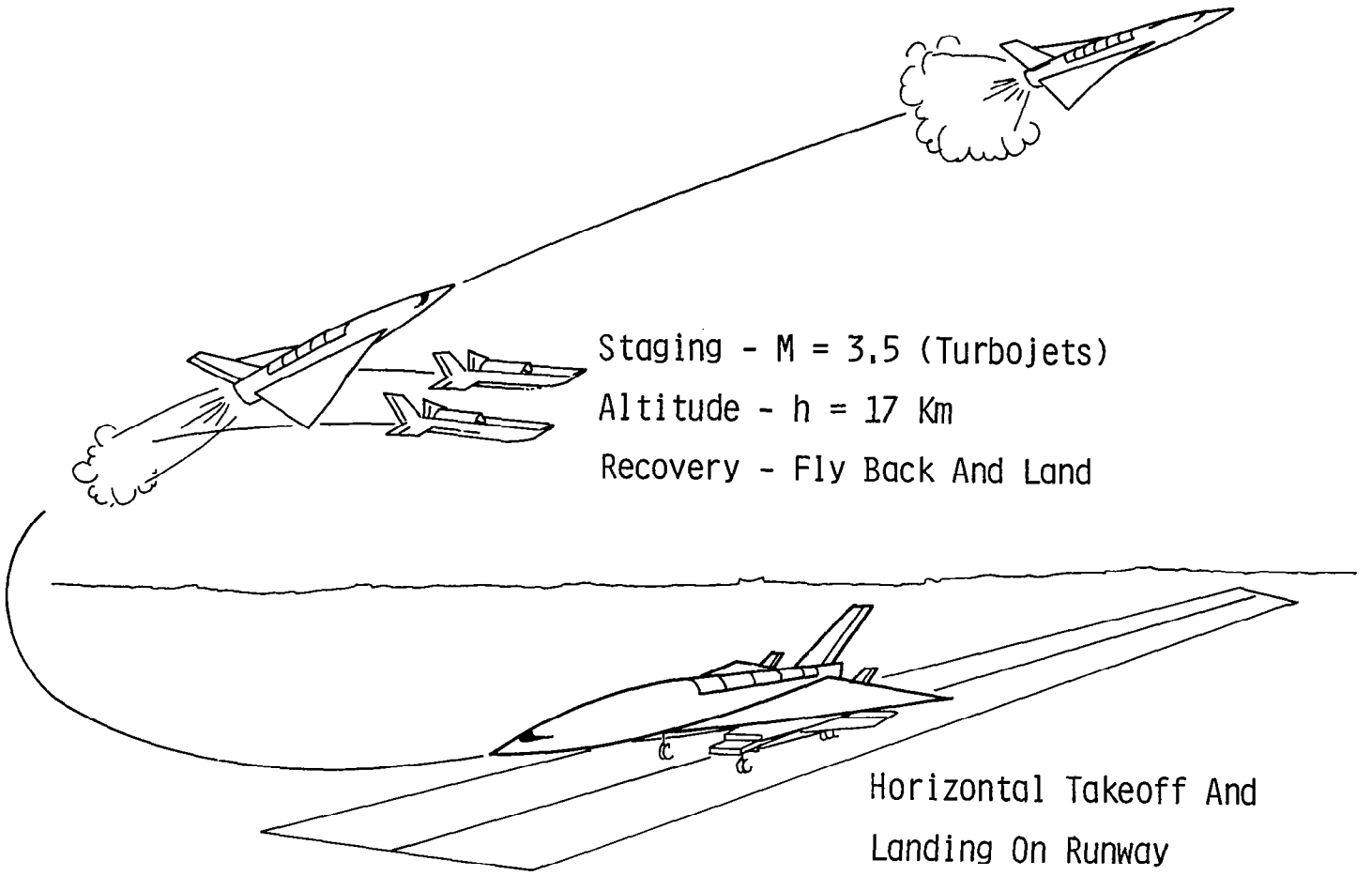

Figure 1.-Turbojet-Boosted Orbiter Concept (Spacejet)

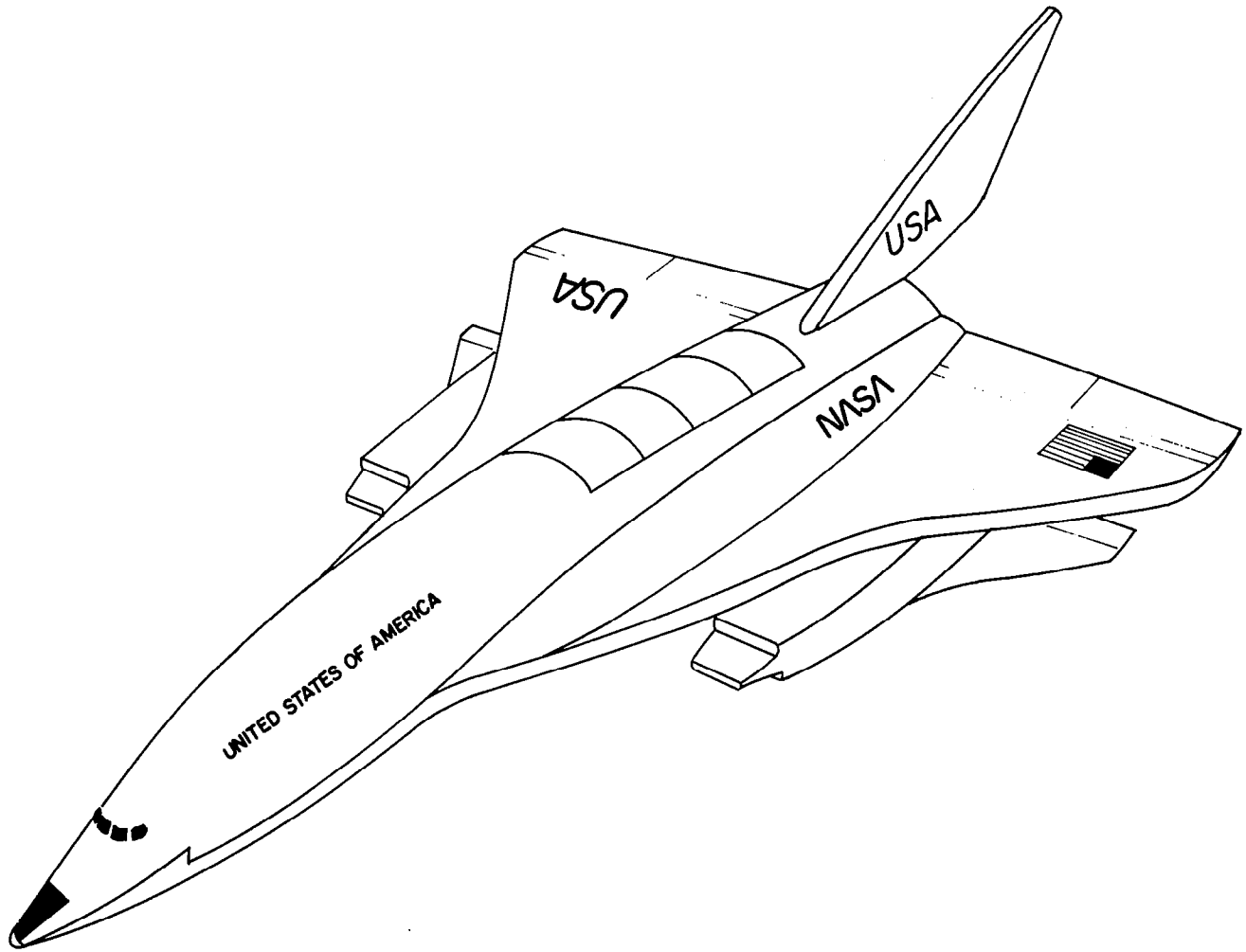

Figure 2.-Spacejet Conceptual Design.

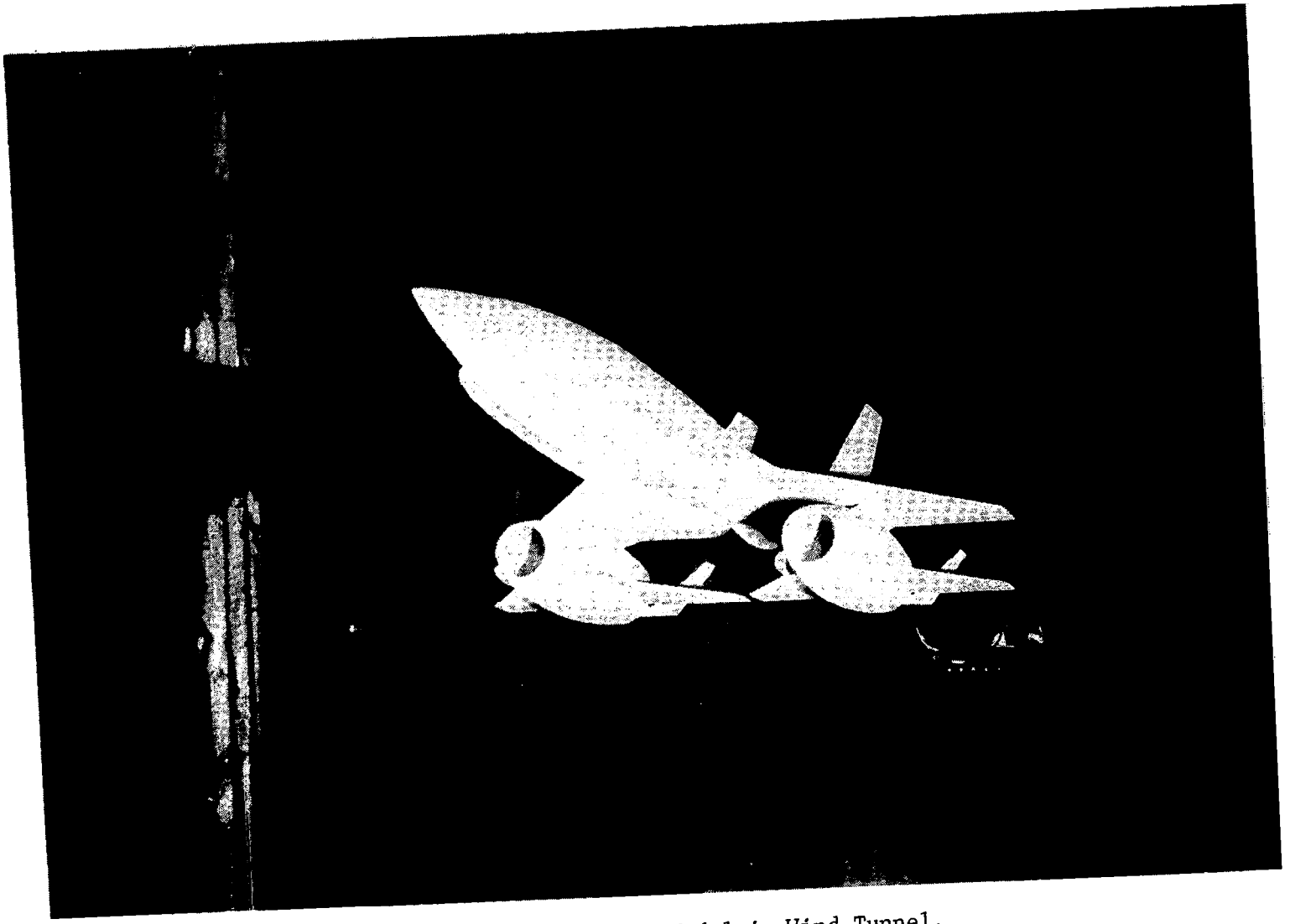

Figure 3.-NASA Spacejet Model in Wind Tunnel.

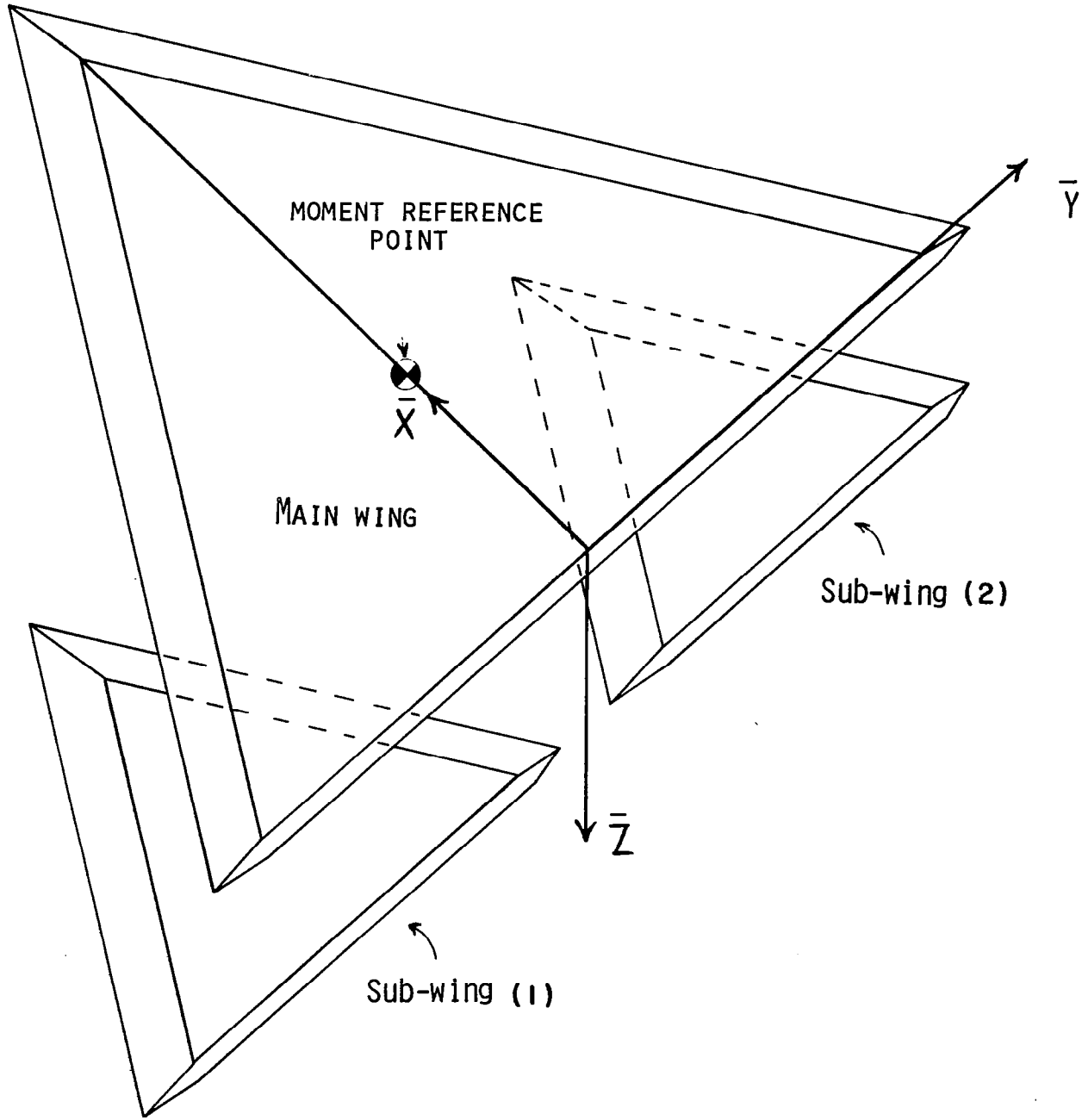

Figure 4.-Coordinate System for USMA Model.

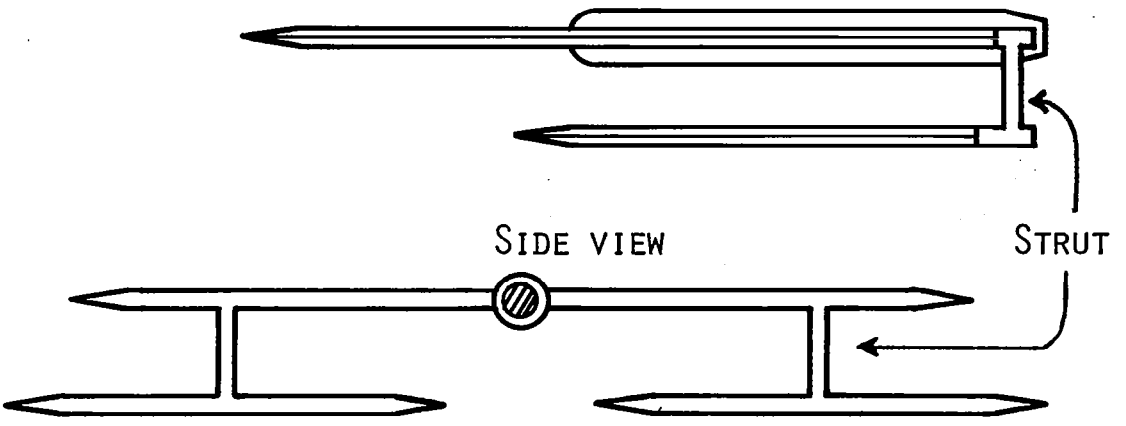

REAR VIEW

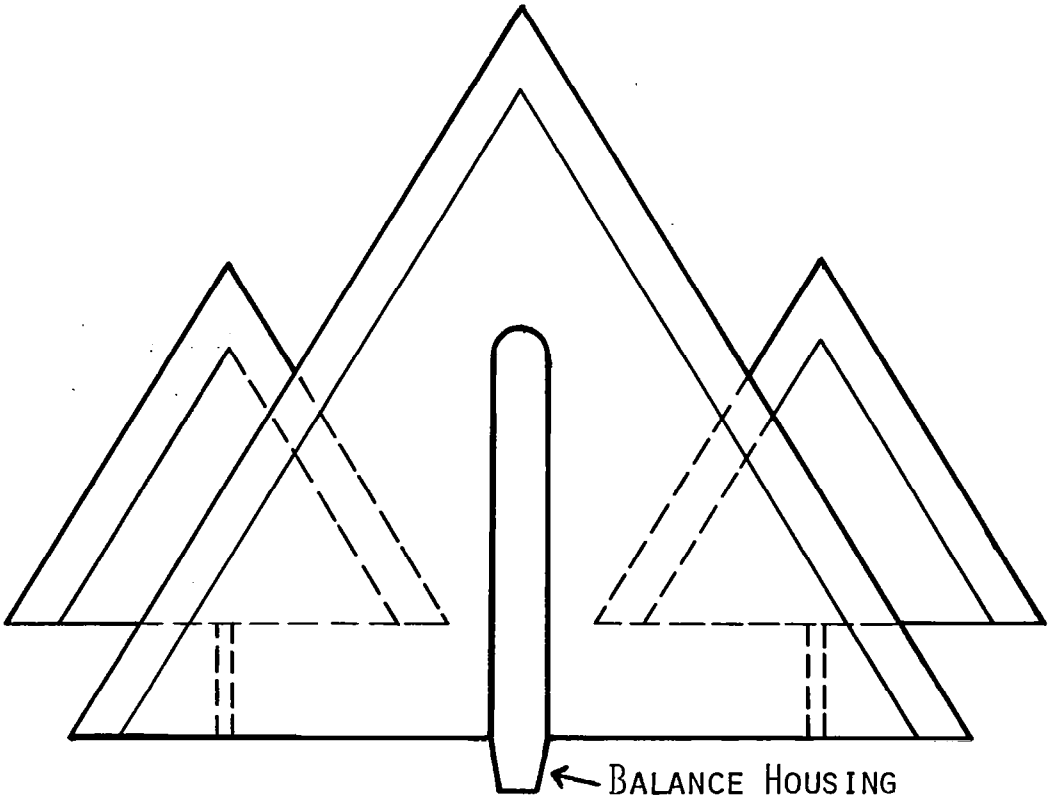

TOP VIEW

Figure 5.-Sketch of USMA Wind Tunnel Model
(X = .1925, Y = .0481, Z = .0962)

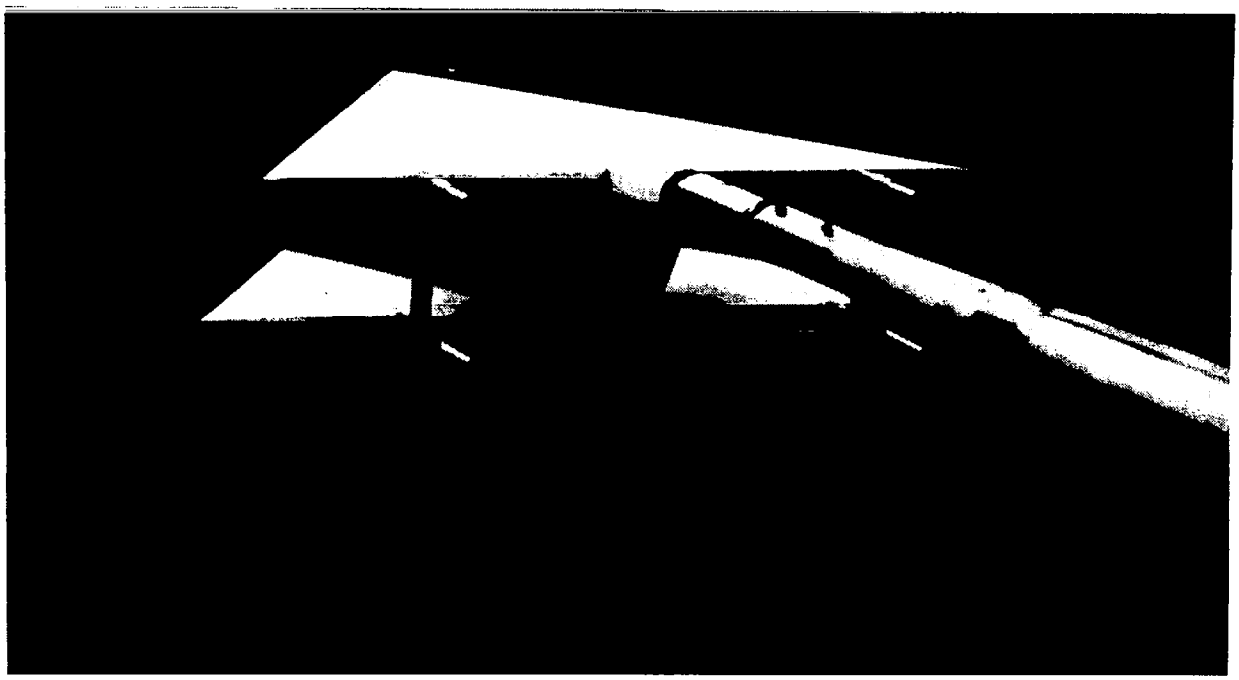

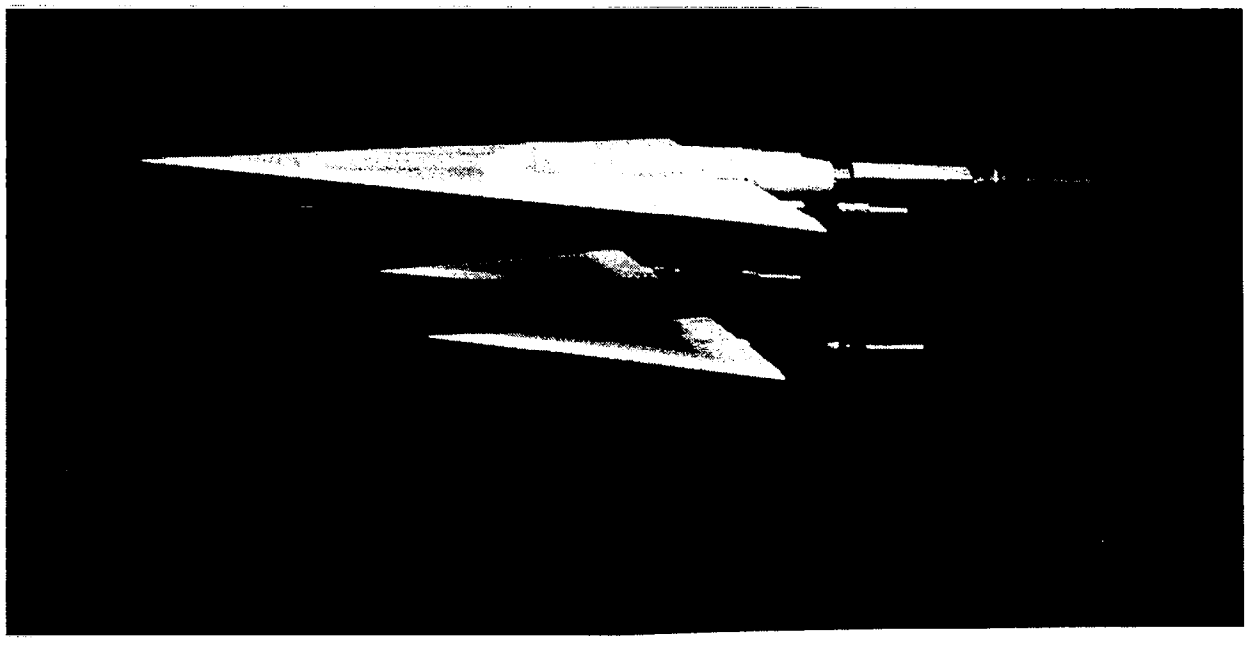

Figure 6.-Typical installation of USMA model in Wind Tunnel:
X = .0962, Y = .1925, Z = .3849.

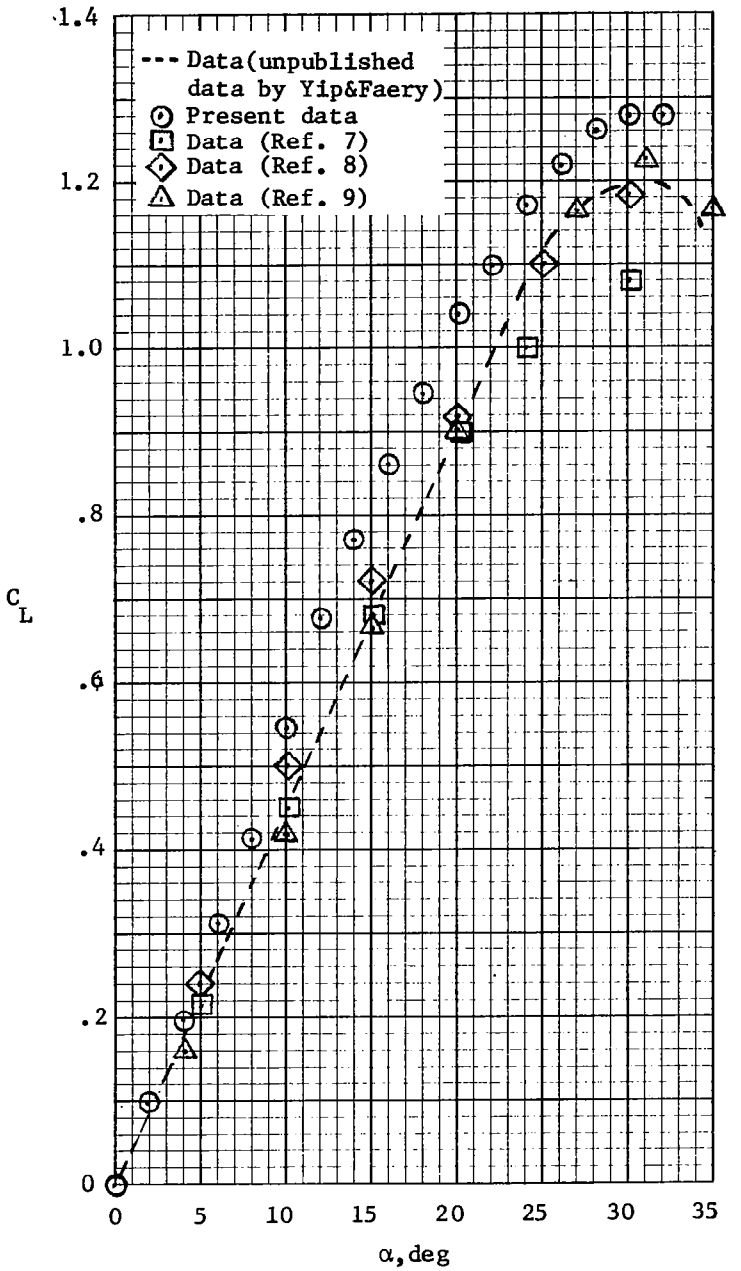

Figure 7.-Lift curves for planar 60° delta wing at $M_\infty \approx 0$.

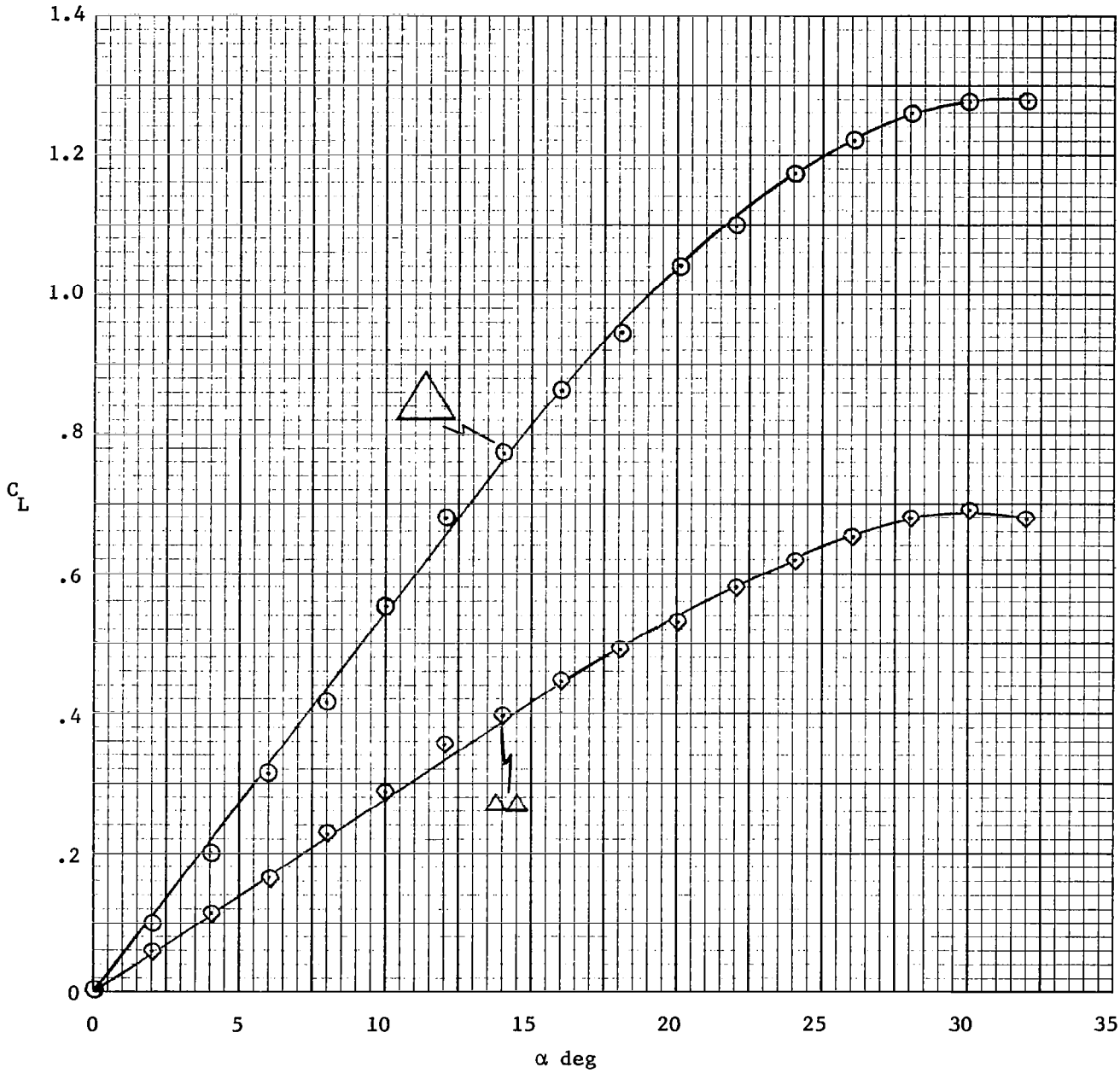

Figure 8.-Lift curves for planar 60° delta main wing alone, and 60° delta sub-wings alone at $M_\infty \approx 0$: Y = 0.

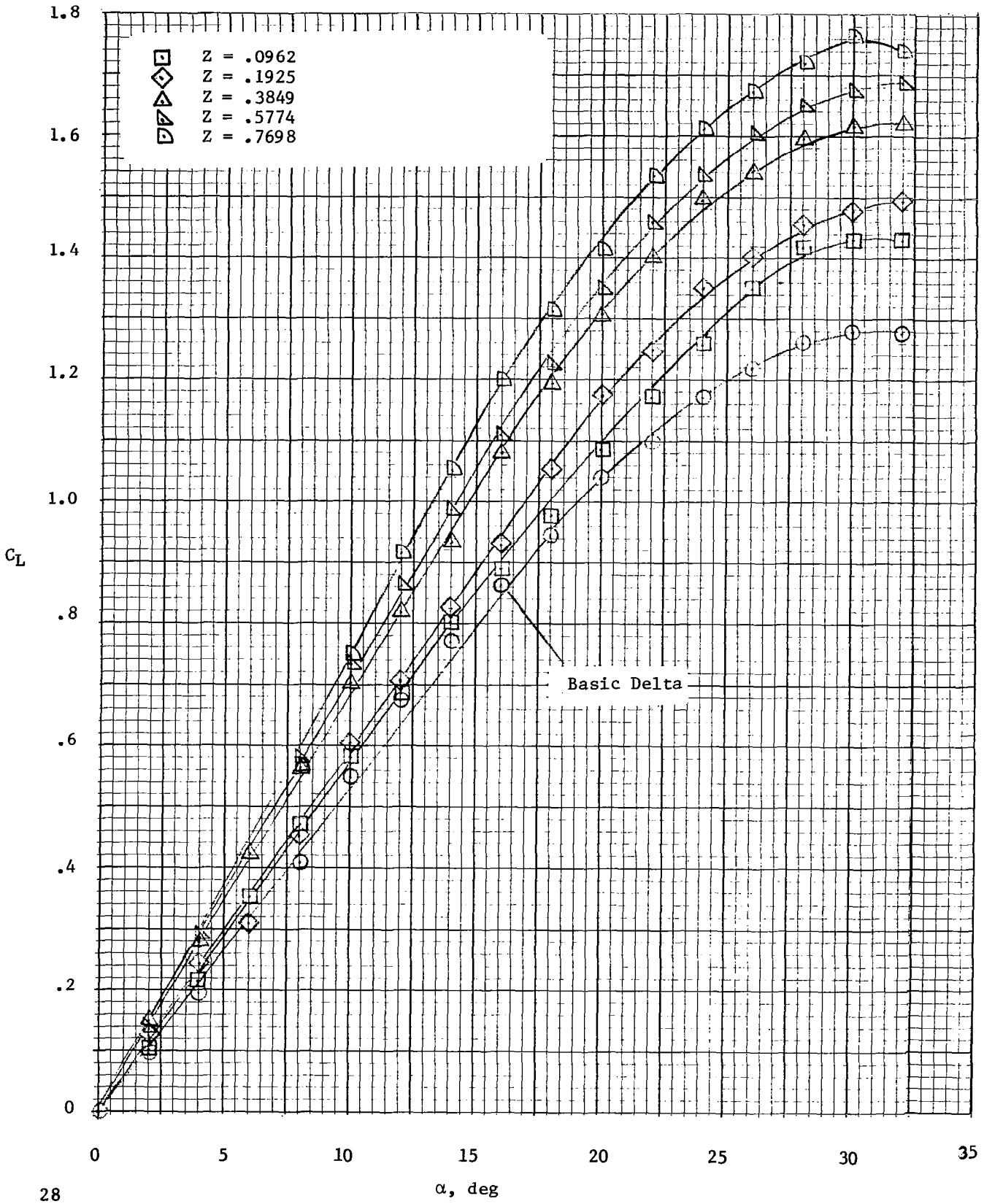

(a) Lift

Figure 9.-Effect of vertical separation on longitudinal aerodynamic characteristics of combination at M_∞ = 0.13: X = 0, Y = 0.

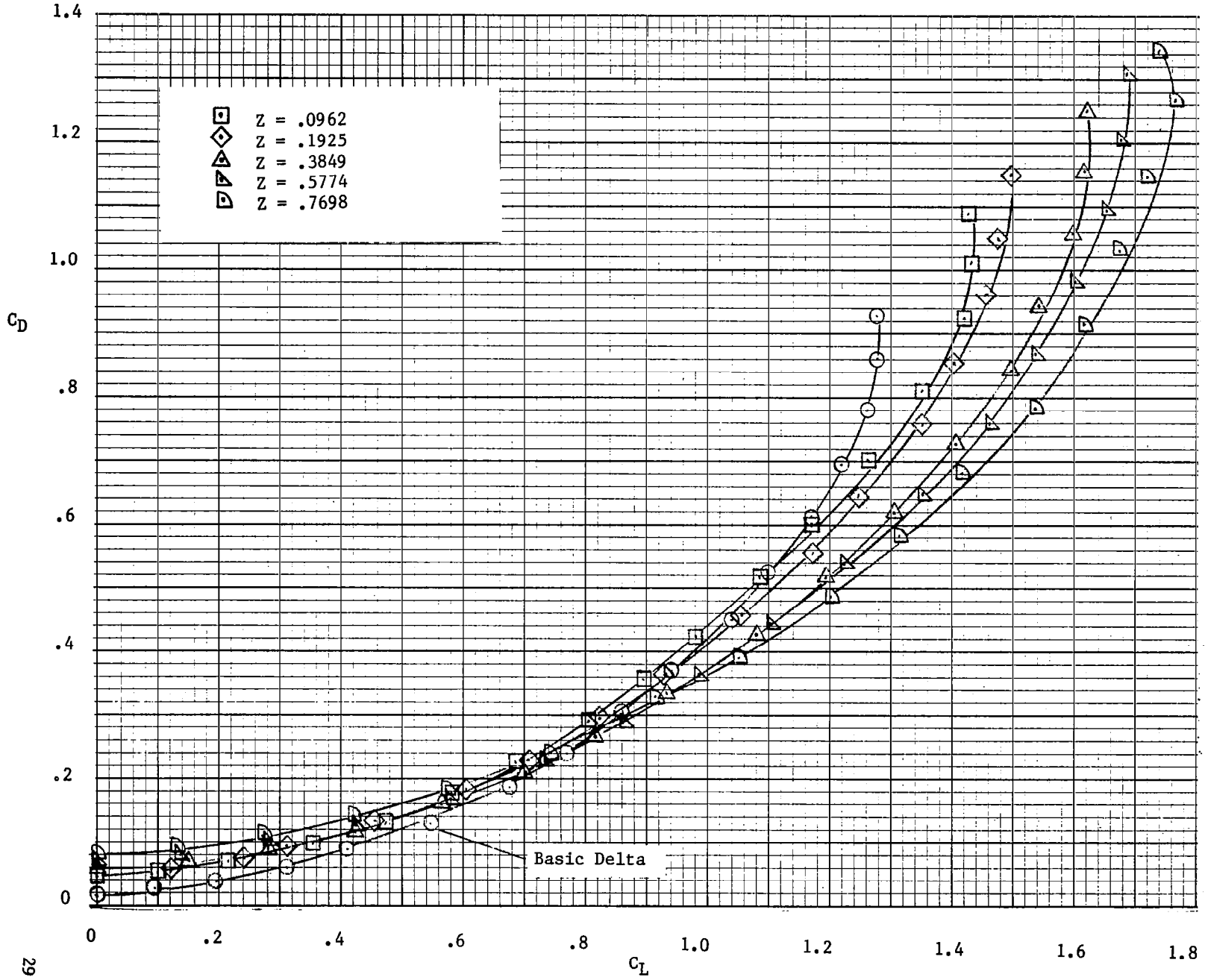

(b) Drag

Figure 9.-Continued.

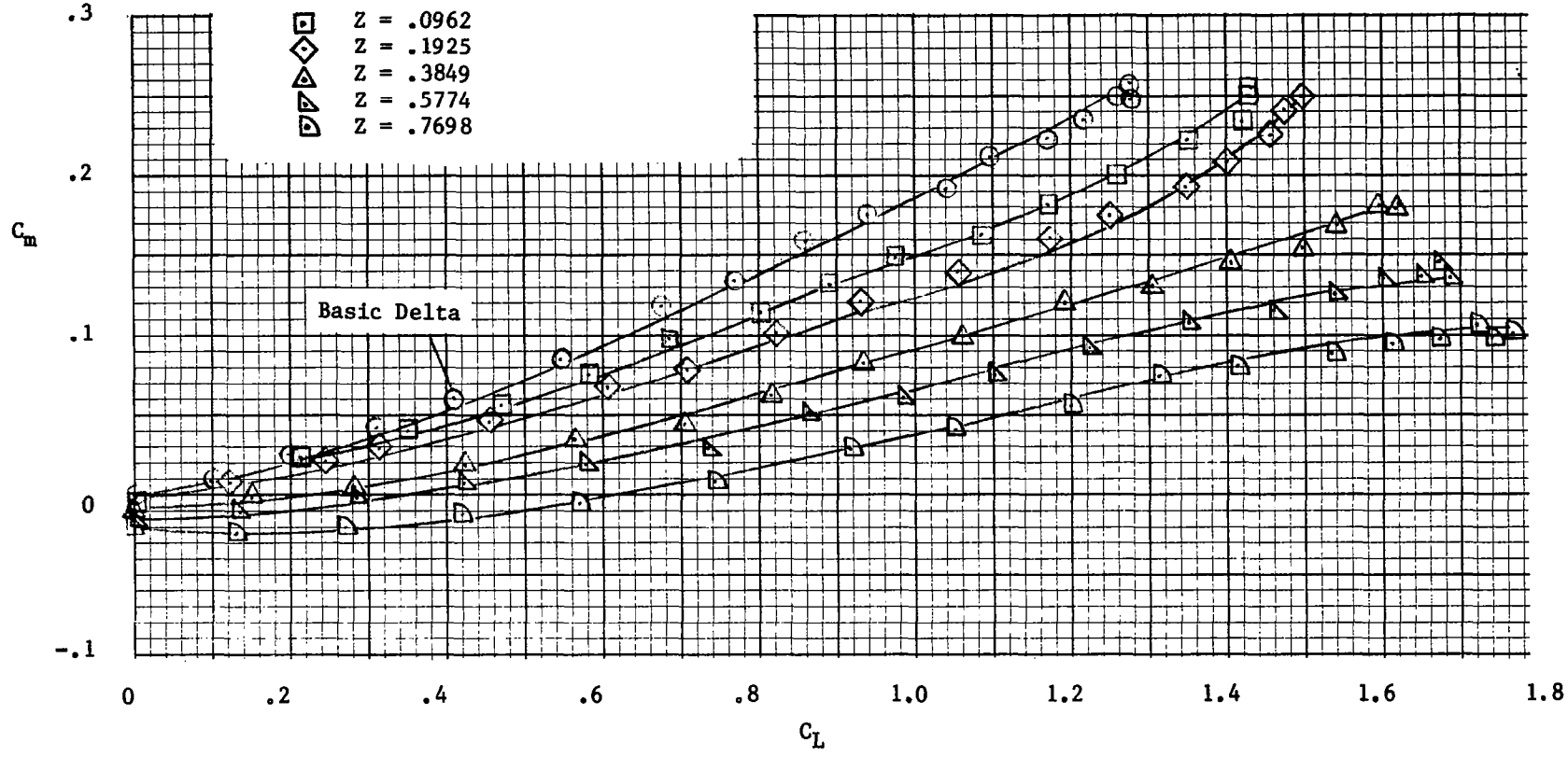

(c) Pitching Moment

Figure 9.-Concluded.

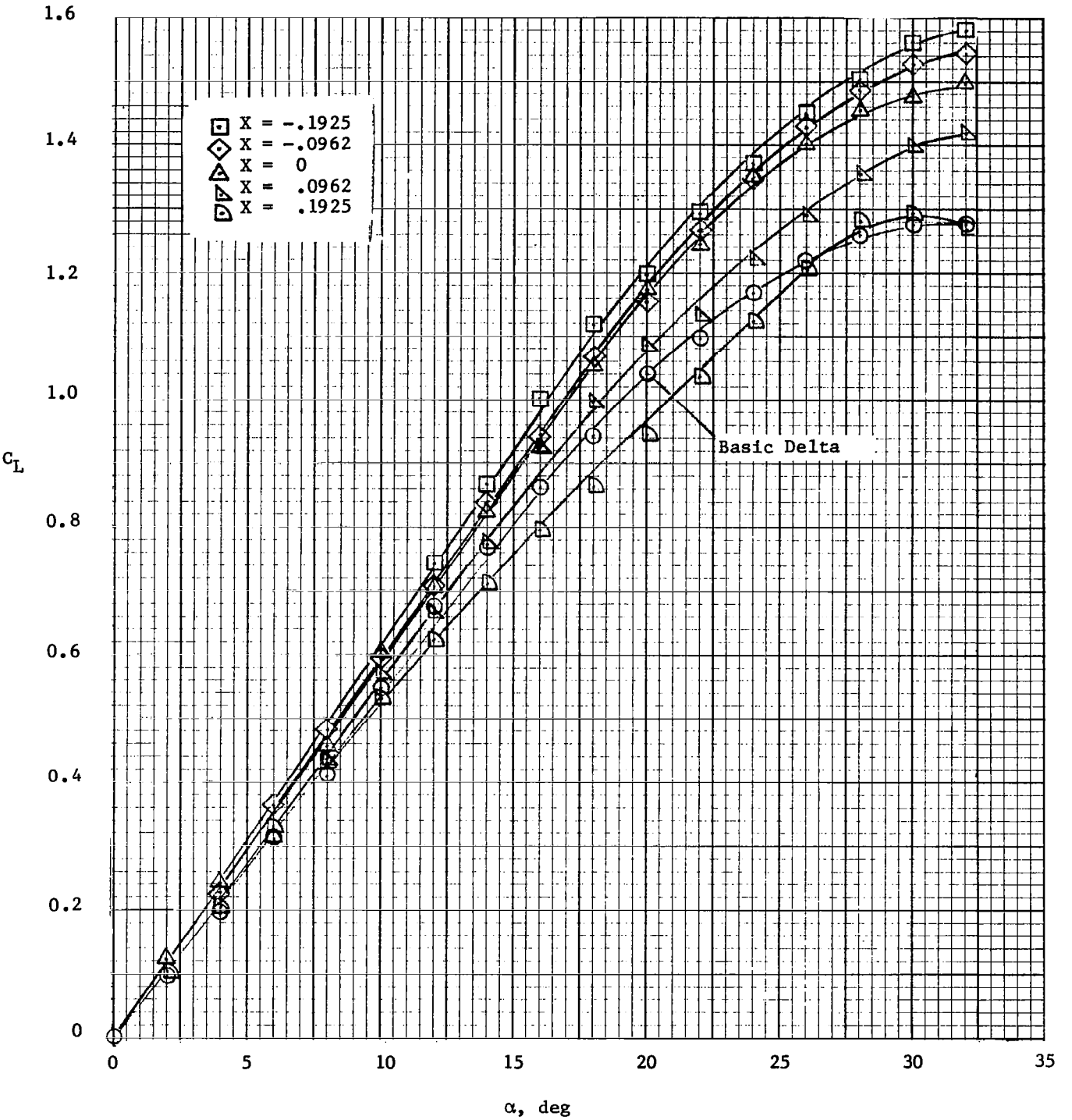

(a) Lift

Figure 10.-Effect of longitudinal position on longitudinal aerodynamic characteristics of configuration at M_∞ = 0.13: Y = 0, Z = .1925.

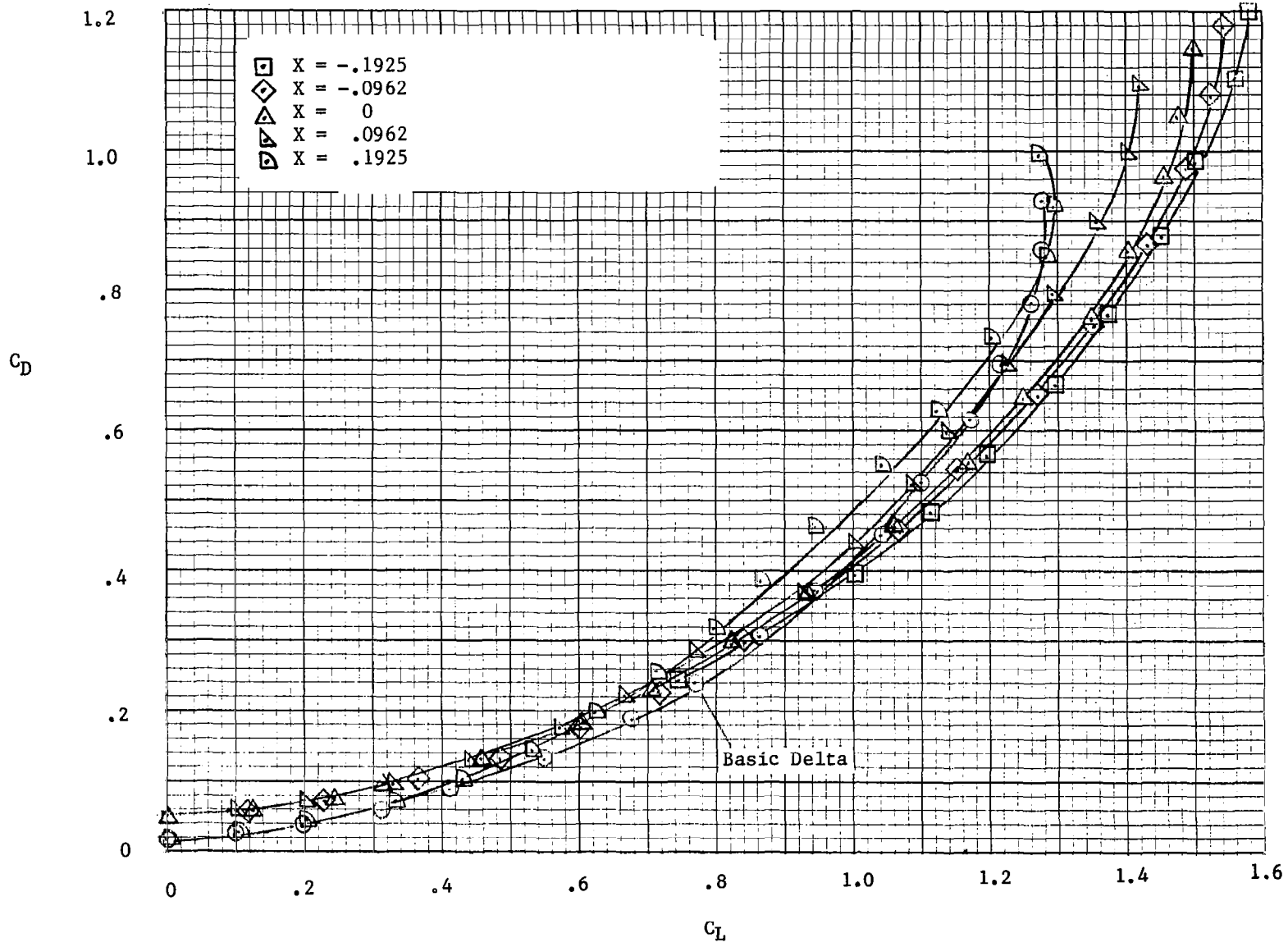

(b) Drag

Figure 10-.Continued.

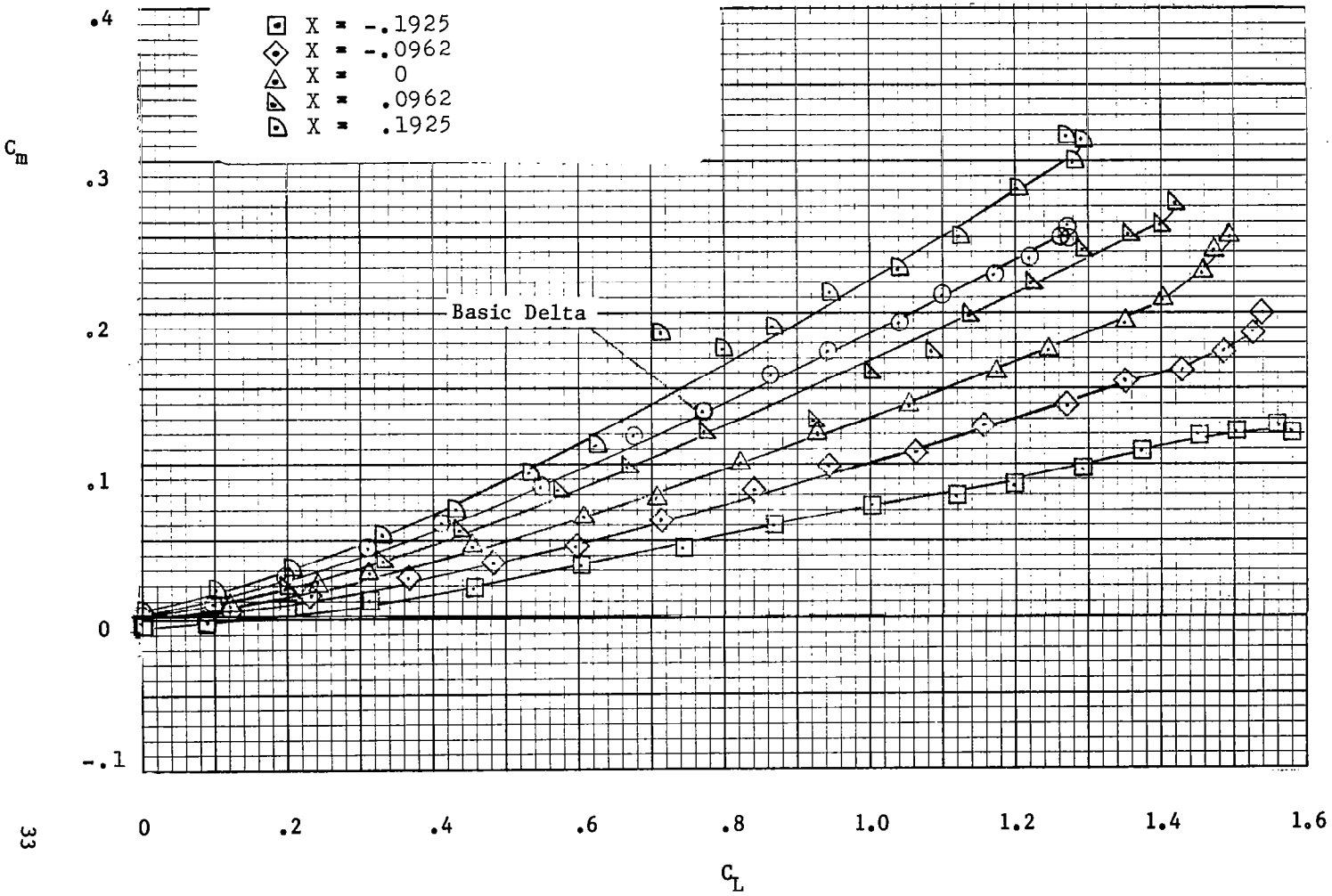

(c) Pitching Moment

Figure 10.-Concluded.

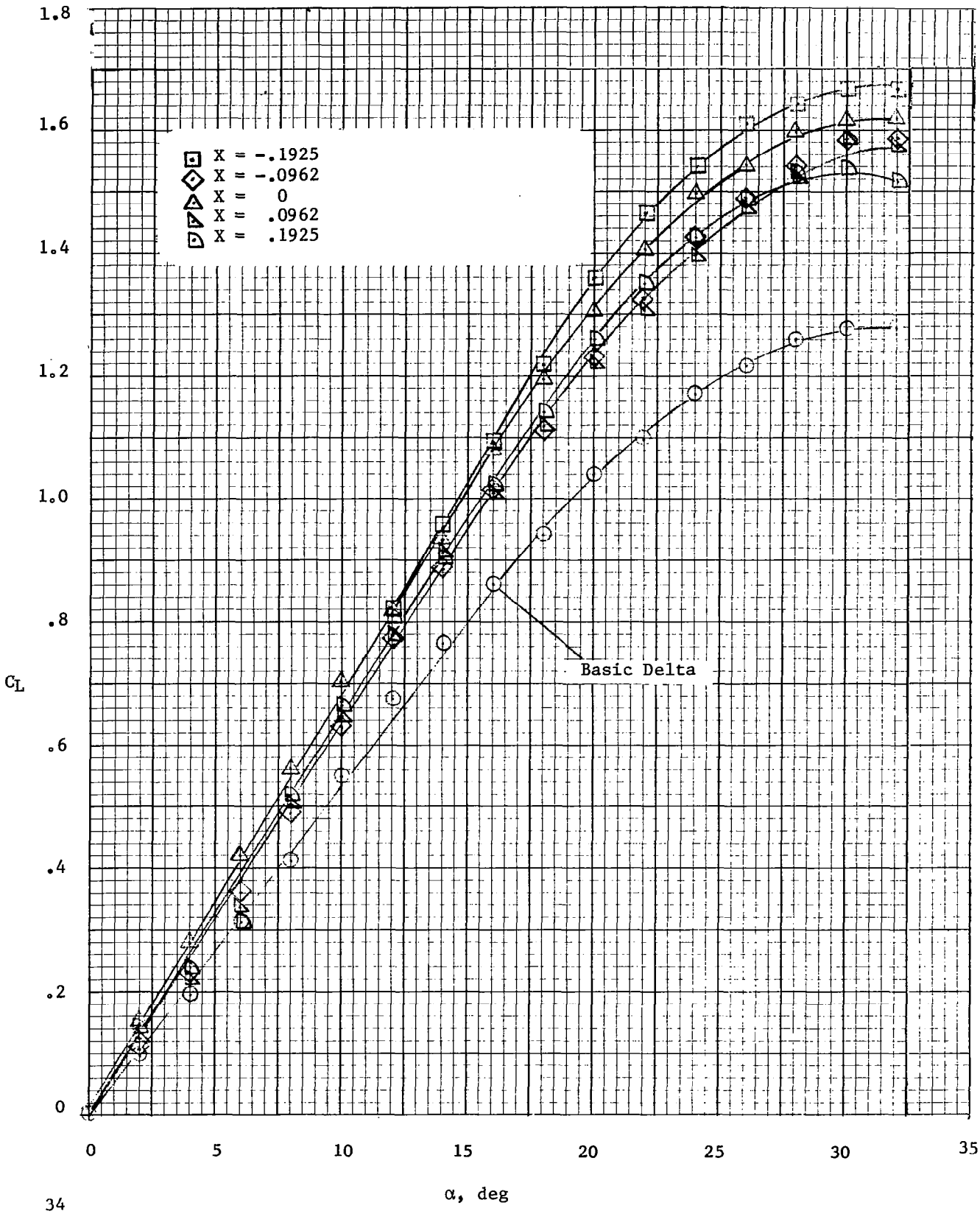

(a) Lift

Figure 11.-Effect of longitudinal position on longitudinal aerodynamic characteristics of configuration at M_∞ = 0.13: Y = 0, Z = .3849.

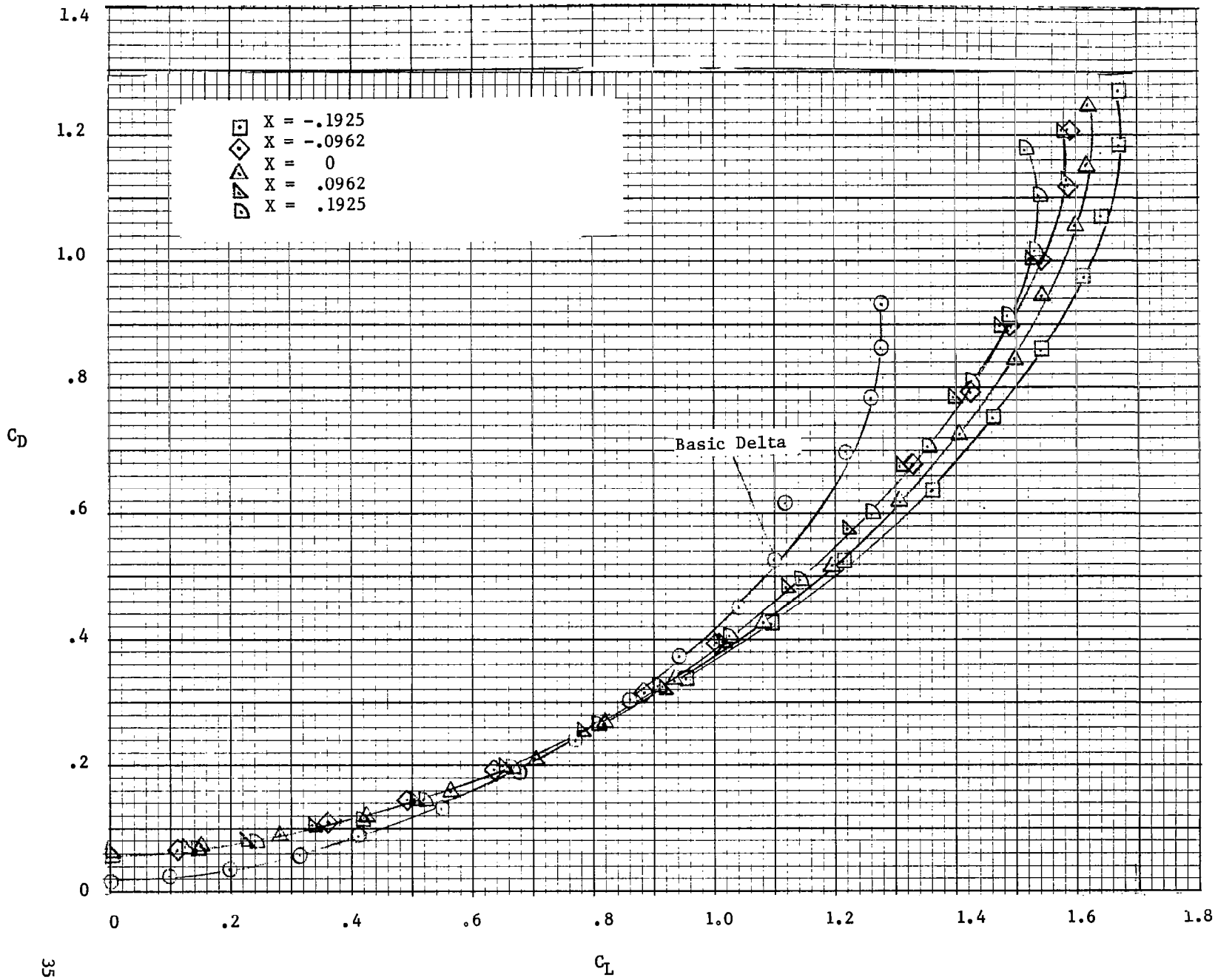

(b) Drag

Figure 11.-Continued.

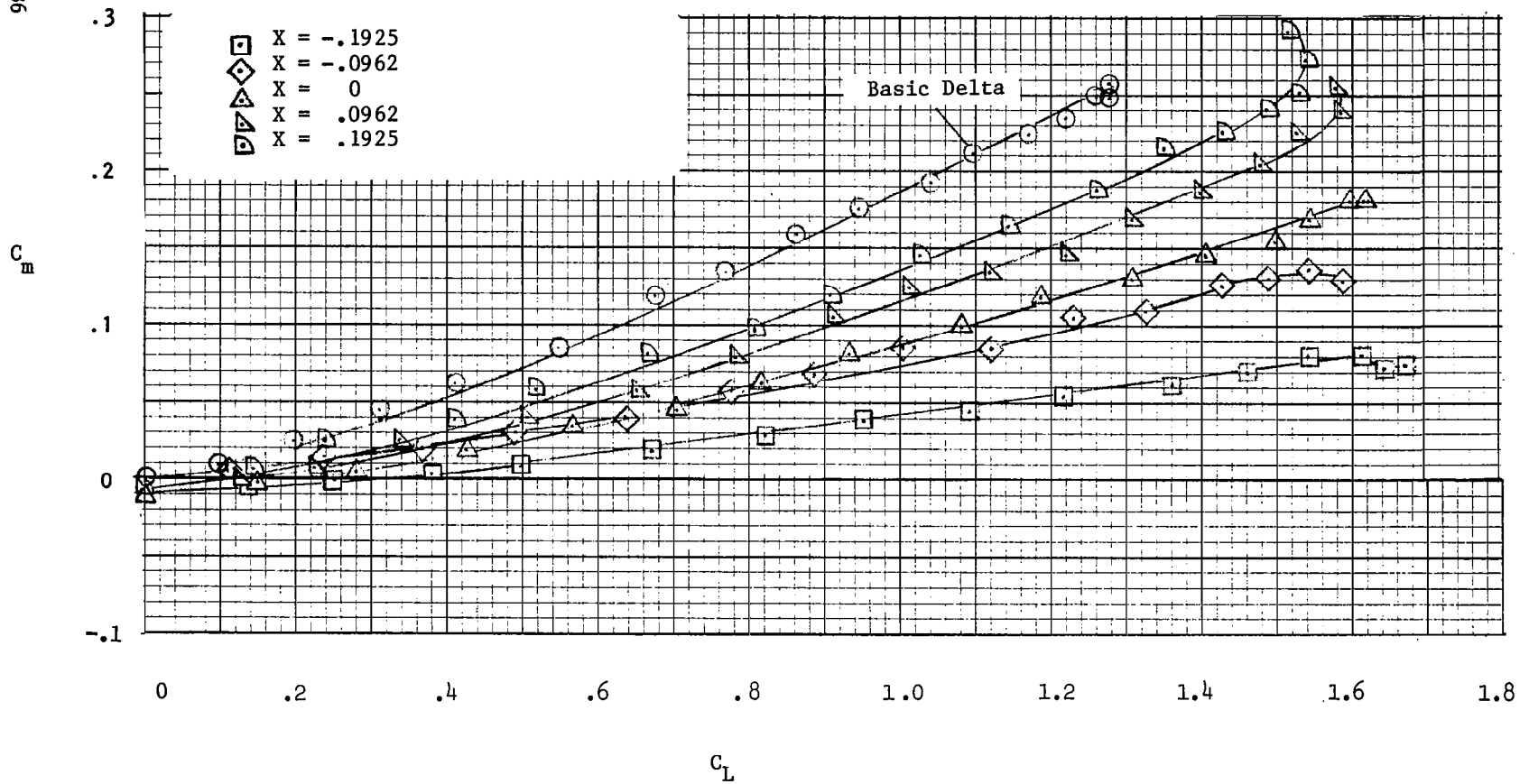

(c) Pitching Moment

Figure 11.-Concluded.

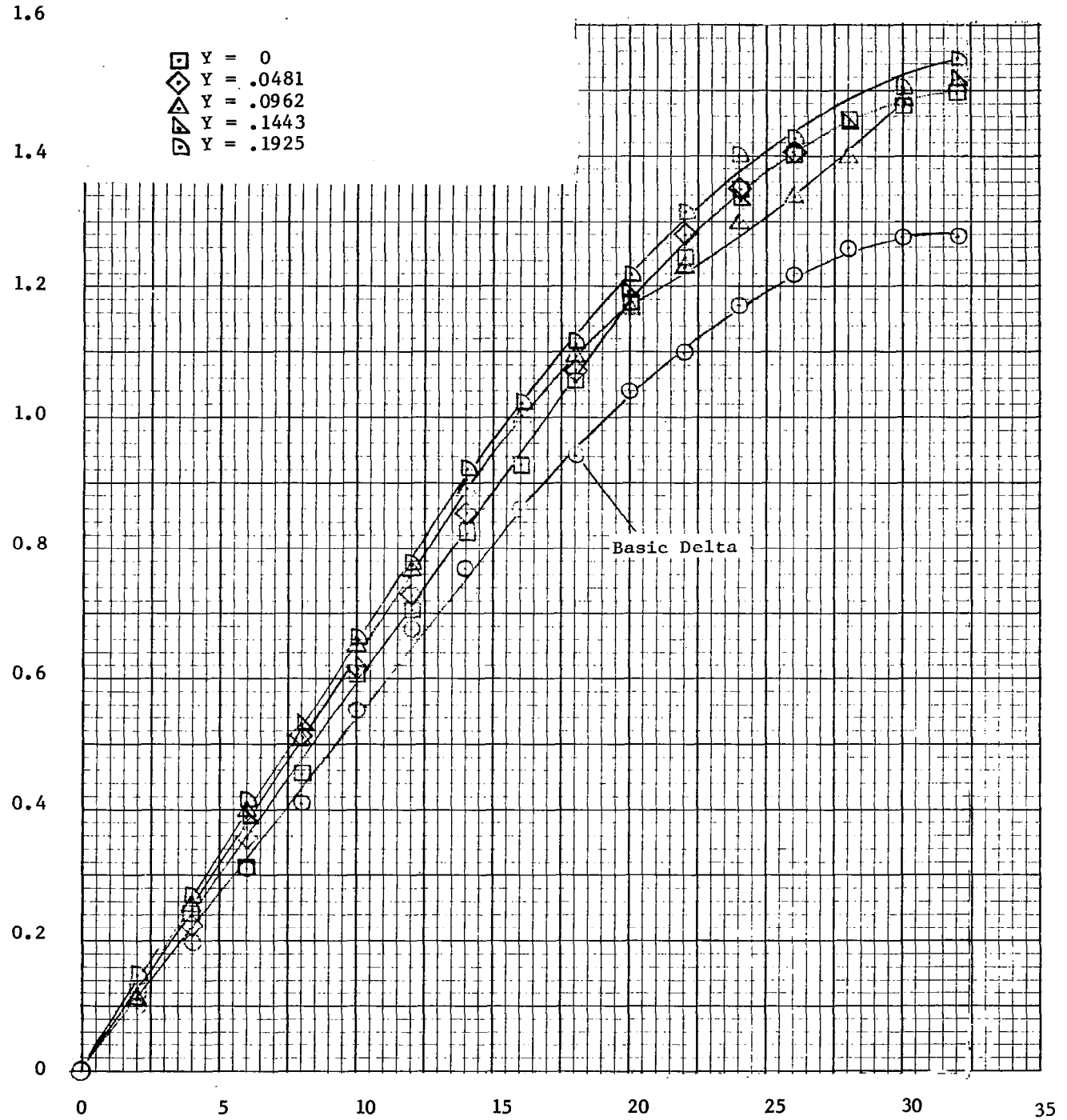

(a) Lift

Figure 12.-Effect of lateral separation on longitudinal aerodynamic characteristics of configuration at M_∞ = 0.13: X = 0, Z = .1925.

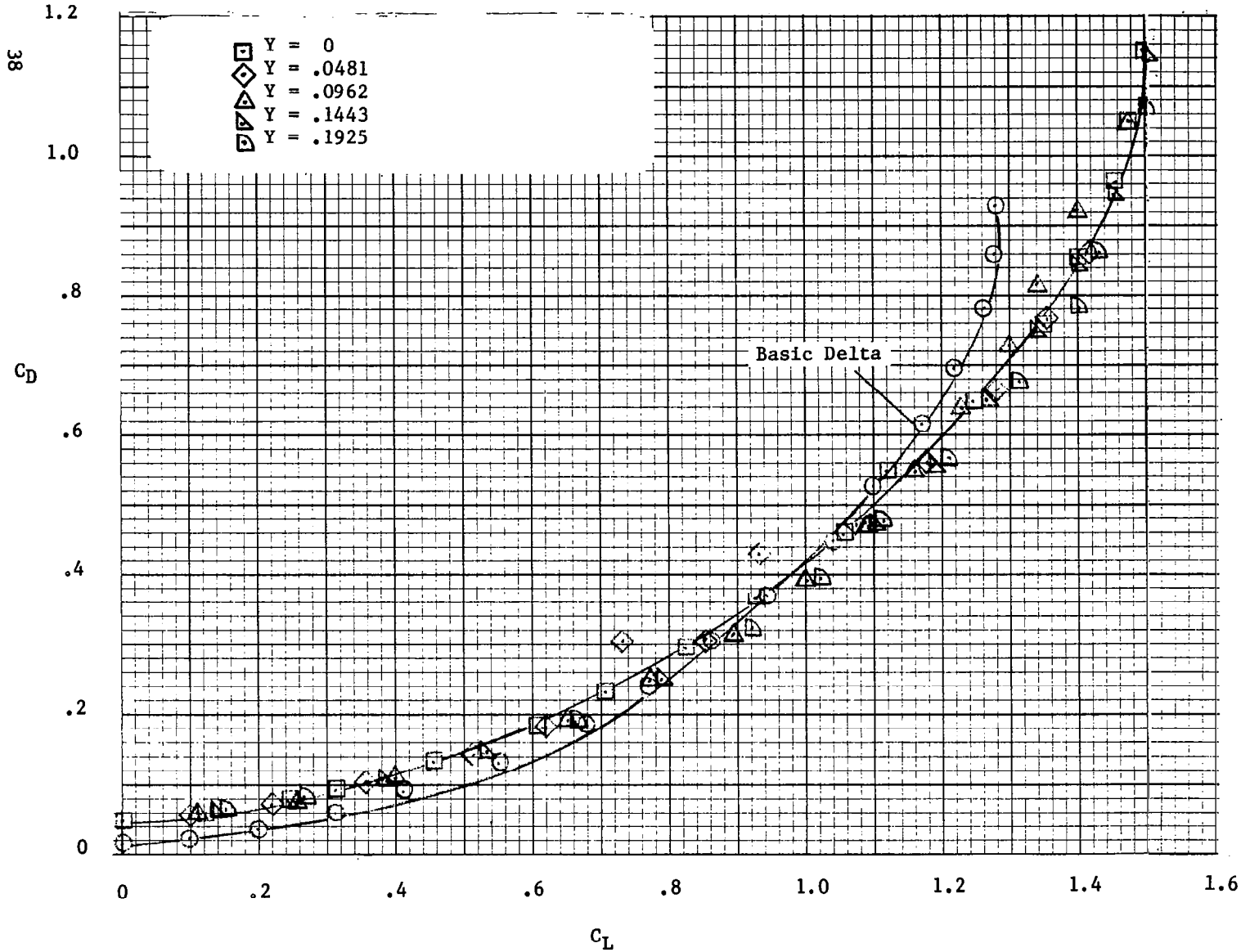

(b) Drag

Figure 12.-Continued.

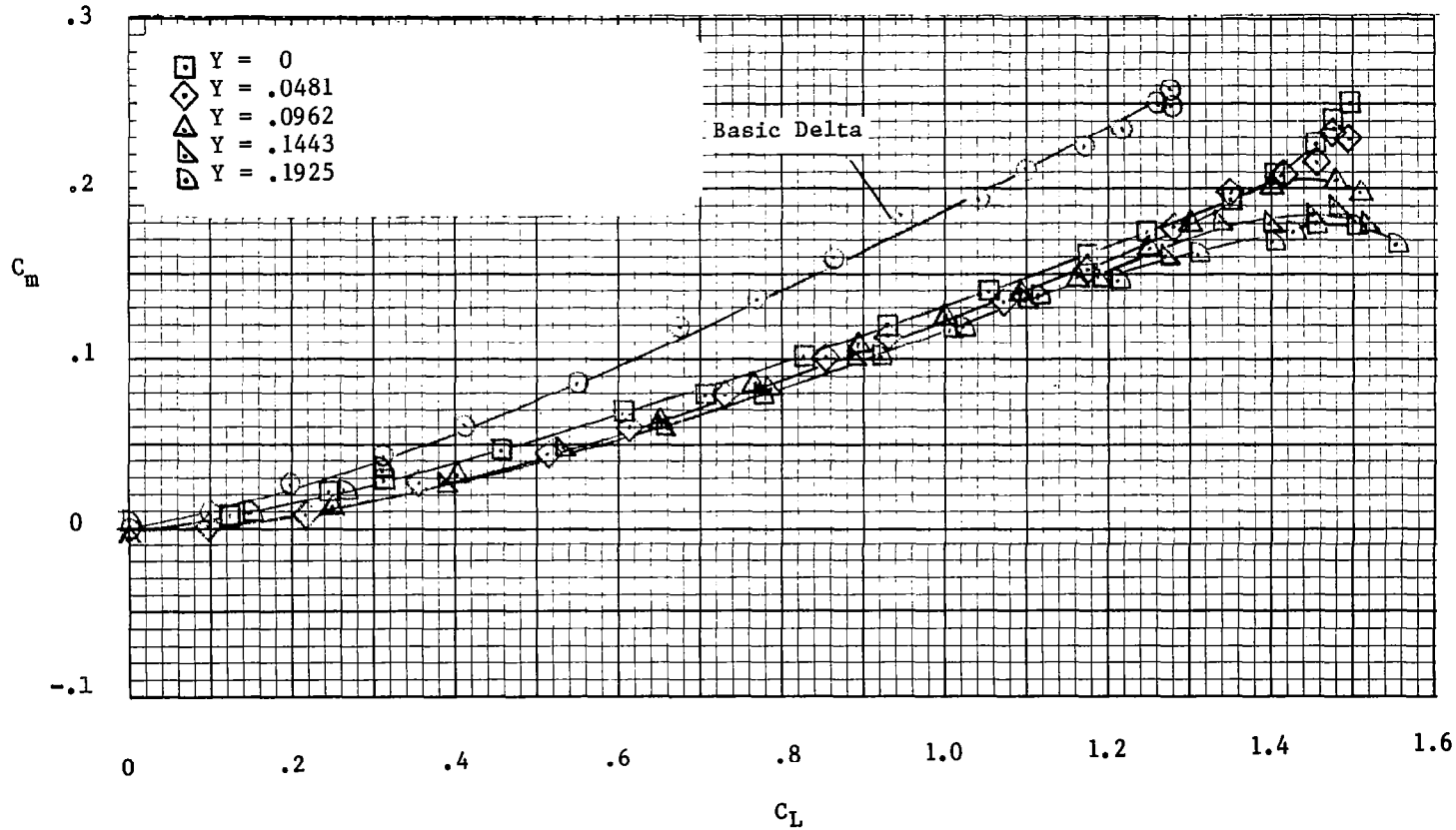

(c) Pitching Moment

Figure 12.-Concluded.

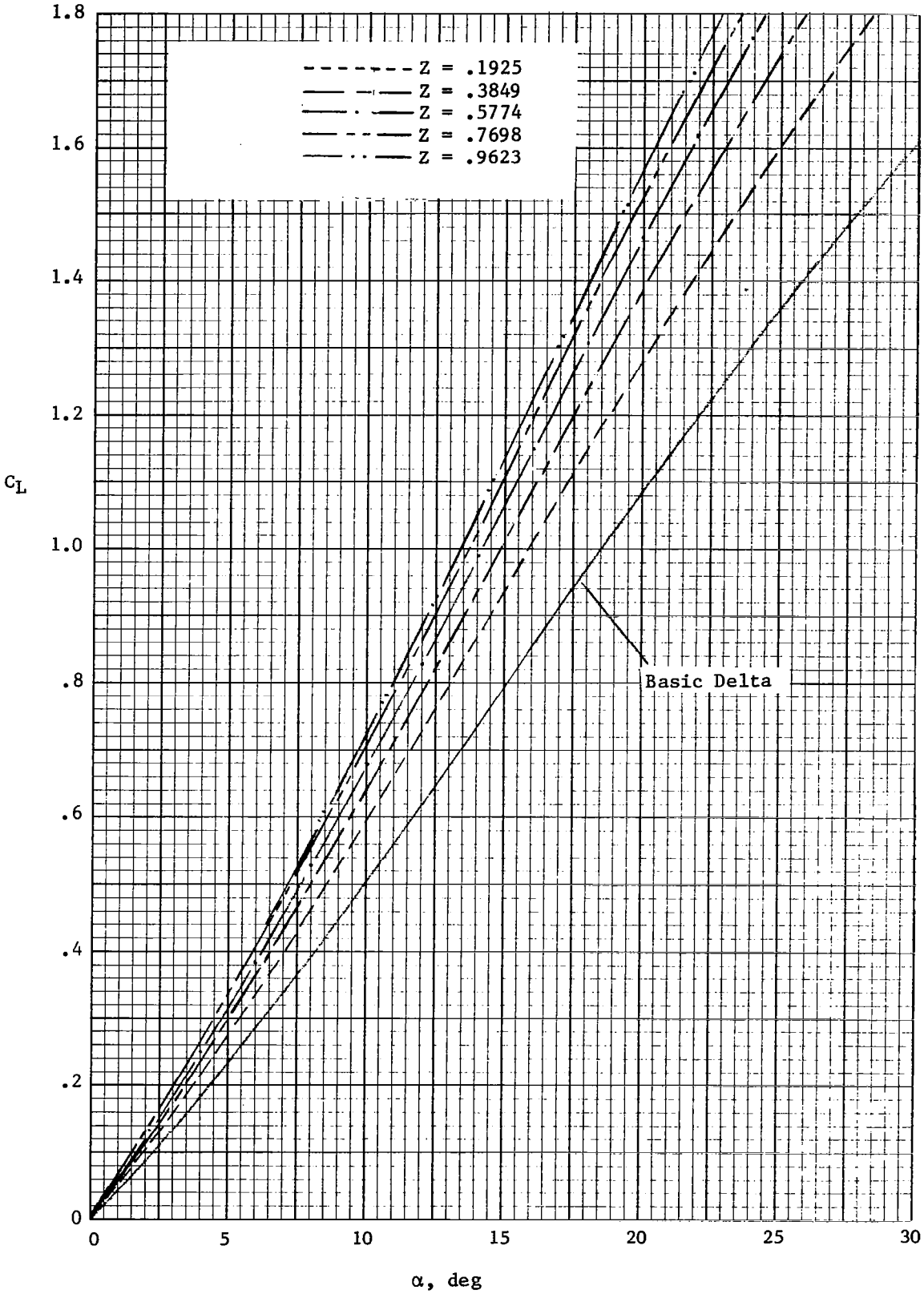

Figure 13.-Effect of vertical separation on the lift curve of the configuration at $M_\infty \approx 0$: X = 0, Y = 0. (Based on VLM theory)

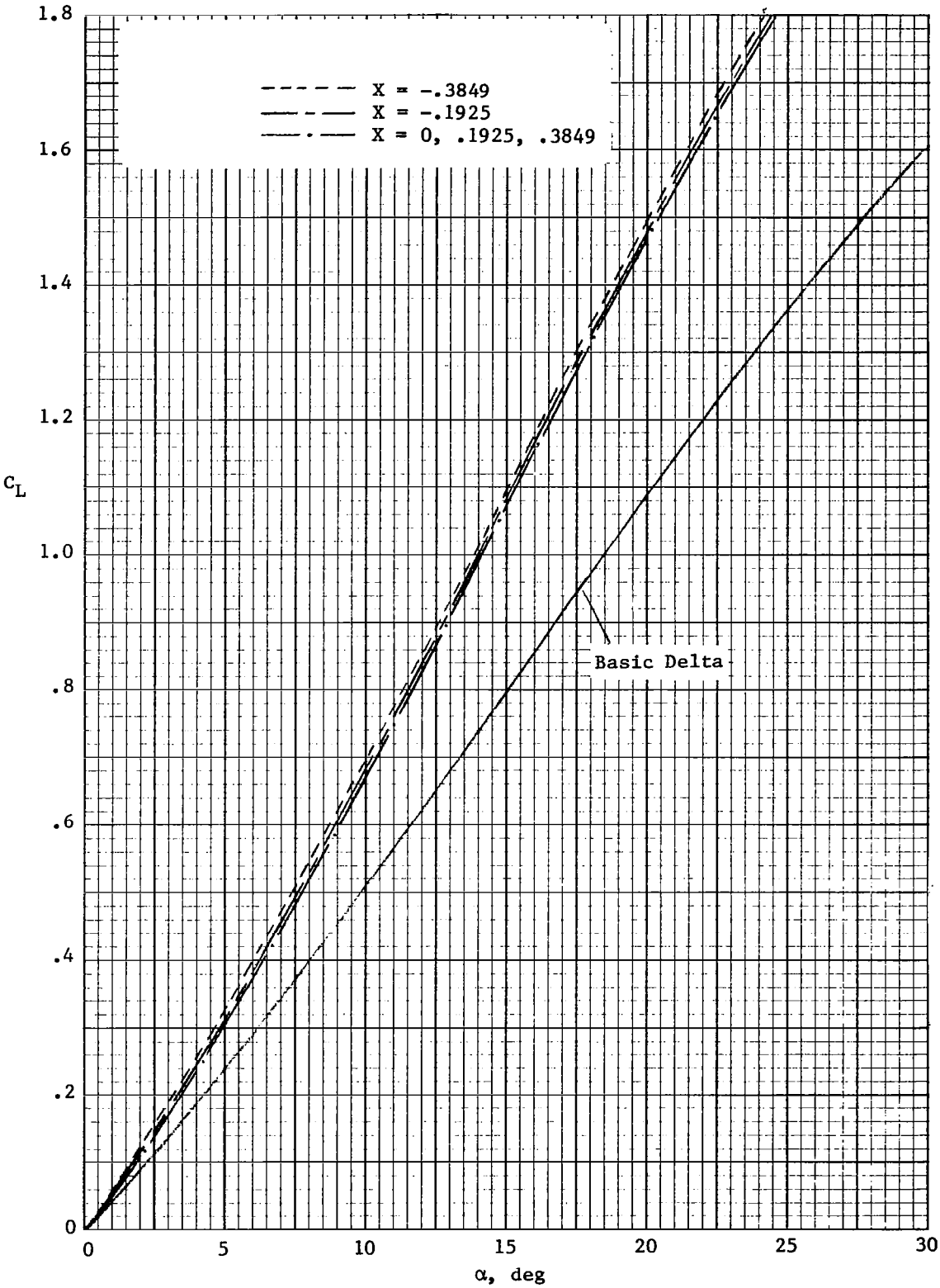

Figure 14.-Effect of longitudinal position on the lift curve of the configuration at $M_\infty \approx 0$: Y = 0, Z = .5774. (Based on VLM theory)

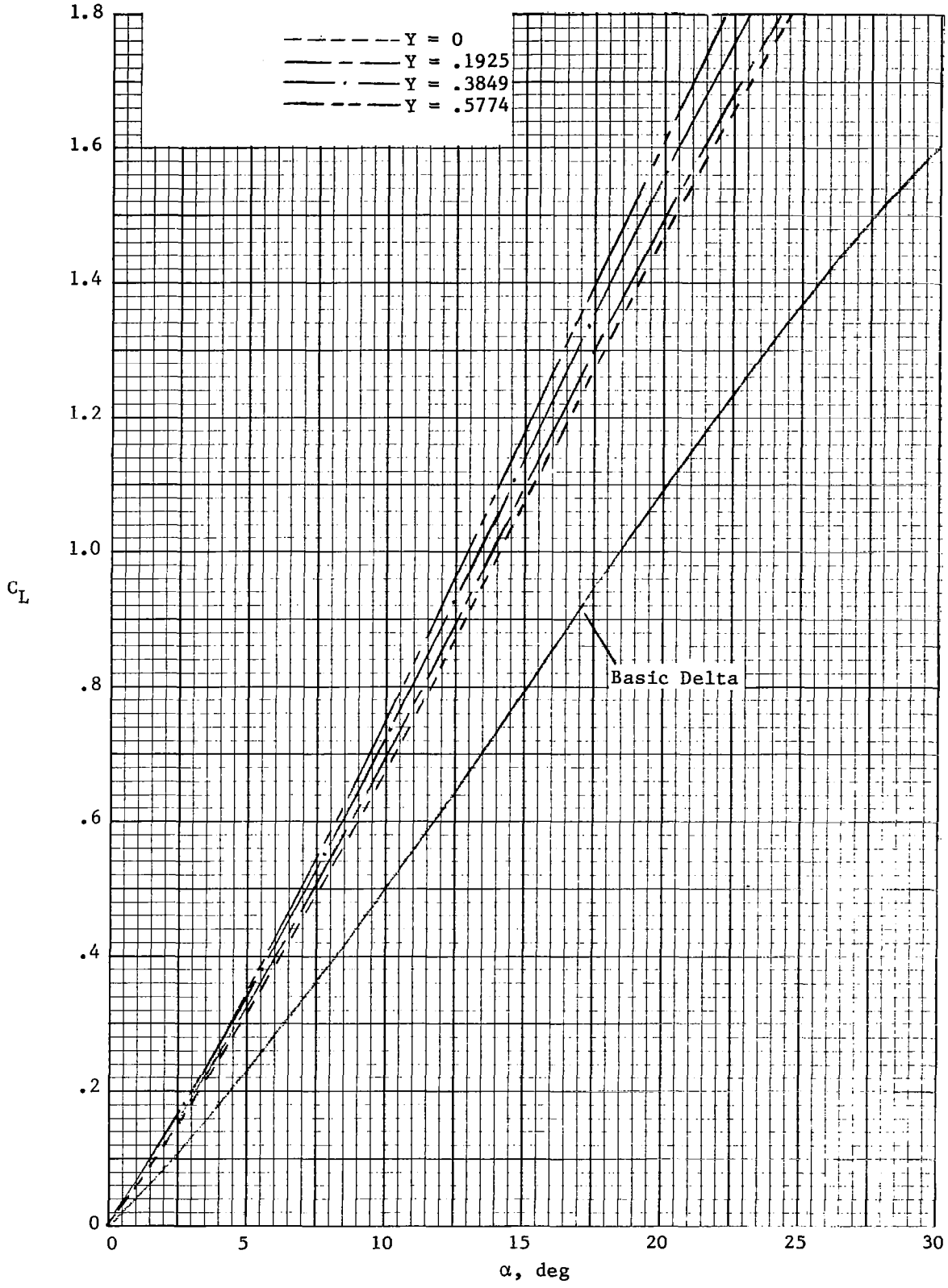

Figure 15.-Effect of lateral separation on lift curve of the configuration at $M_\infty \approx 0$: X = 0, Z = .5774. (Based on VLM theory)

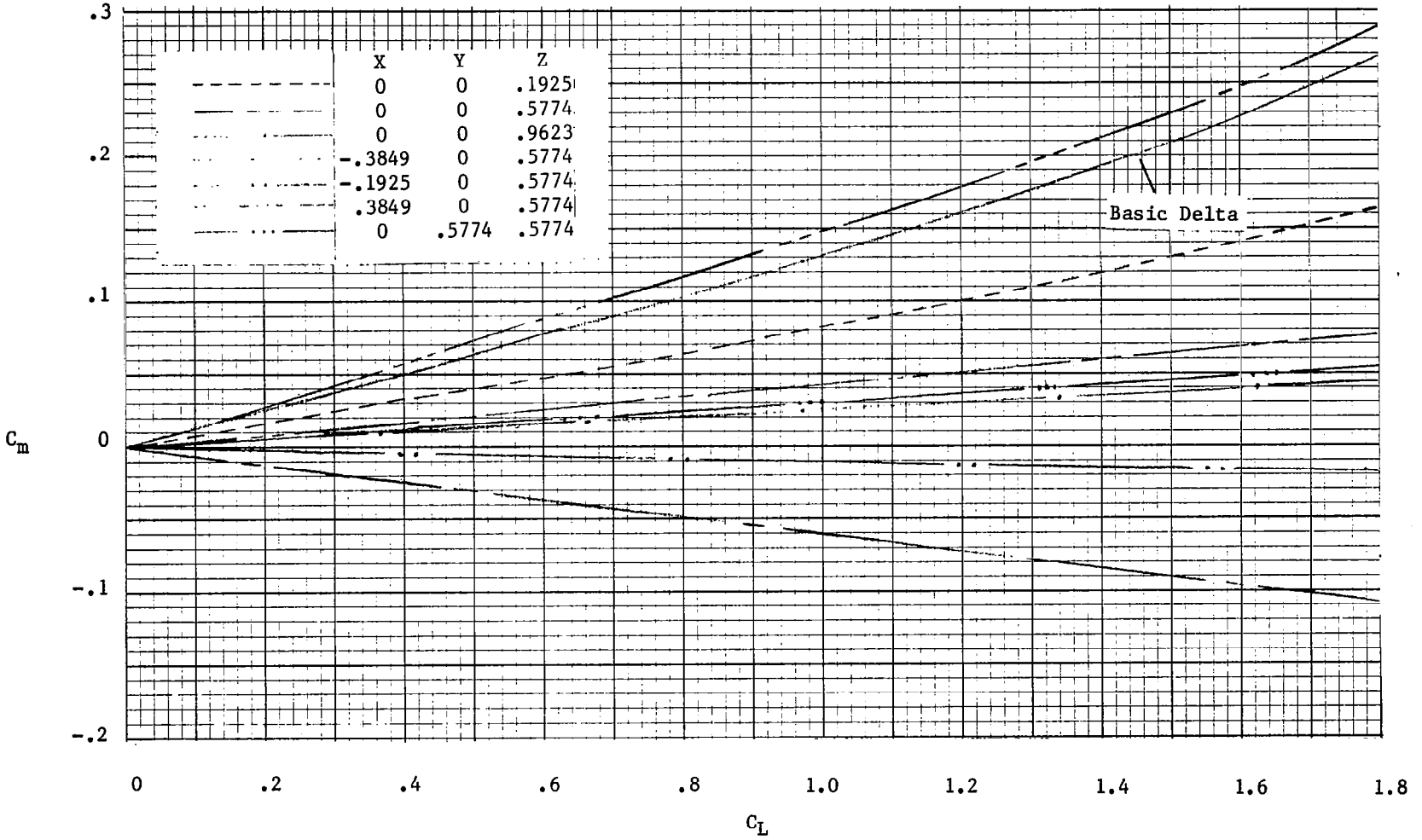

Figure 16.-Effect of configuration changes on pitching moment at $M_\infty \approx 0$. (Based on VLM theory)

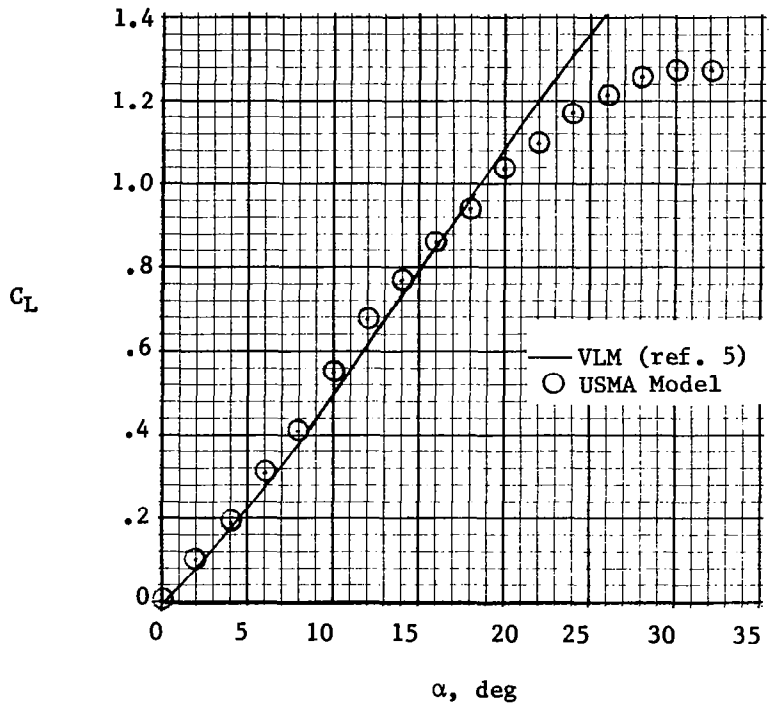

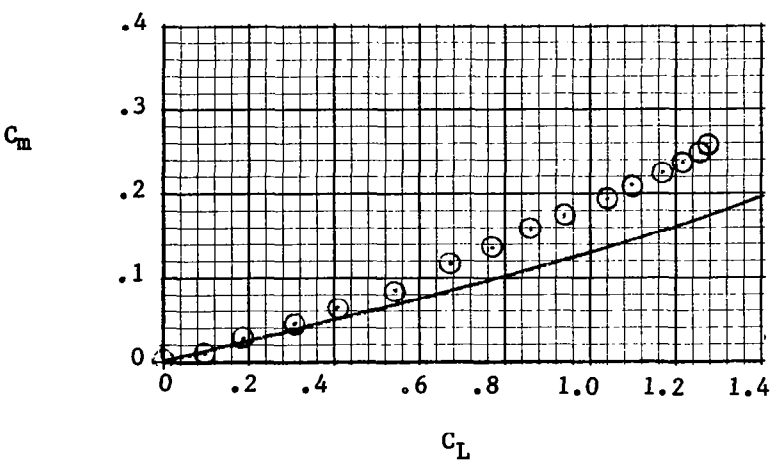

Figure 17.-Longitudinal results for 60° delta wing at $M_\infty \approx 0$.

1. Report No.	2. Government Accession No.	3. Recipient's Catalog No.
NASA CR-3460		

4. Title and Subtitle	5. Report Date
EXPERIMENTAL AND THEORETICAL STUDY OF THREE INTERACTING, CLOSELY-SPACED, SHARP-EDGED 60° DELTA WINGS AT LOW SPEEDS	October 1981
	6. Performing Organization Code

7. Author(s)	8. Performing Organization Report No.
H. F. Faery, Jr., J. K. Strozier, and J. A. Ham	
	10. Work Unit No.

9. Performing Organization Name and Address	11. Contract or Grant No.
Department of Mechanics United States Military Academy West Point, New York 10996	
	13. Type of Report and Period Covered
12. Sponsoring Agency Name and Address	Contractor Report
National Aeronautics and Space Administration Washington, DC 20546	14. Sponsoring Agency Code

15. Supplementary Notes

This report was prepared in cooperation with NASA Langley Research Center and funded by the United States Military Academy
Langley Technical Monitor: John E. Lamar

16. Abstract

Wind tunnel tests have been conducted at the US Military Academy to determine the subsonic longitudinal aerodynamic characteristics of a unique lifting configuration. It consisted of a thin 60° delta main wing with two, also thin, smaller 60° delta wings (called sub-wings here) attached underneath. The test was designed to determine the effects on lift, drag, and pitching moment due to various placement of the sub-wings in relation to the main wing. Test results indicate that increasing vertical separation between the main wing and the sub-wings produced the most significant results; a 23.1% increase in maximum lift coefficient, a reduction in drag coefficient at high lift coefficients, and an increase in longitudinal stability. Lateral separation of the sub-wings produced no significant changes. Placement of the sub-wings rearward increases the initial lift curve slope and maximum lift coefficient and also increases the longitudinal stability. Results of a computer study using a NASA-developed vortex lattice code supported the experimental conclusions.

17. Key Words (Suggested by Author(s))	18. Distribution Statement
Delta wing Vortex lift	Unclassified-Unlimited Subject Category 02

19. Security Classif. (of this report)	20. Security Classif. (of this page)	21. No. of Pages	22. Price
Unclassified	Unclassified	45	A03

For sale by the National Technical Information Service, Springfield, Virginia 22161

NASA-Langley, 1981